

MASTER OF BIOSTATISTICS
NATIONAL AND KAPODISTRIAN UNIVERSITY OF ATHENS
MEDICAL SCHOOL
DEPARTMENT OF MATHEMATICS

DIPLOMA THESIS
ANASTASIA TSIOGKA

**An epidemiological study evaluating contrast
sensitivity change in refractive surgery**

ATHENS, 2020



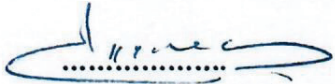
This diploma thesis is submitted in partial fulfilment of the requirements for the degree of
BIOSTATISTICS

that is given by the Medical School and the Department of Mathematics of the National
and Kapodistrian University of Athens.

It was approved on _____ by the thesis examining committee:

NAME

SIGNATURE

- | | | |
|-----------------------|--|---|
| 1. SAMOLI EVANGELIA | Assistant Professor of Epidemiology and
Medical Statistics, National and Kapodistrian
University of Athens | 
..... 24/2/2021 |
| 2. KARMIRIS EFTHYMIOS | Consultant Ophthalmologist,
Hellenic Air Force, Athens | 
.....
23 Feb 2021 |
| 3. SPAETH GEORGE L. | Research Professor,
Wills Eye Hospital, Philadelphia | 
.....
20 Feb 2021 |

*TO MY SON MOURATIO
TO MY DAUGHTER IOANNA
AND TO EVERY OTHER DREAM OF MY LIFE THAT WILL COME TRUE*

*“Shall I compare thee to a summer's day?
Thou art more lovely and more temperate.
Rough winds do shake the darling buds of May,
And summer's lease hath all too short a date.
Sometime too hot the eye of heaven shines,
And often is his gold complexion dimmed;
And every fair from fair sometime declines,
By chance, or nature's changing course untrimmed.
But thy eternal summer shall not fade
Nor lose possession of that fair thou ow'st;
Nor shall death brag thou wand'rest in his shade,
When in eternal lines to time thou grow'st,
So long as men can breathe or eyes can see,
So long lives this, and this gives life to thee.”*

Sonnet 18, William Shakespeare

Acknowledgments

I warmly thank the Chief Supervisor of my dissertation, Assistant Professor of Epidemiology and Medical Statistics in the National and Kapodistrian University of Athens, Mrs. Evangelia Samoli, for her decisive role, her valuable contribution at every stage of the elaboration of this work, and the generous contribution of her knowledge and experience. I feel very lucky and grateful for her confidence in achieving this goal.

I would like to express my sincere gratitude to Dr. Karmiris Efthymios, consultant Ophthalmic Surgeon at Hellenic Air Force General Hospital, a member of the three-member advisory committee, for his undivided support, for the inspiration he inspires, for his always appropriate advice and interventions. Without his touching, persistent and generous help, it would have been impossible to complete this dissertation. I consider myself a privileged person who worked under his scientific guidance but also lucky that I have met him personally.

I would also like to express my warm thanks to Dr. George Spaeth, a world-renowned ophthalmologist and Director Emeritus of the Glaucoma Service at Wills Eye Hospital, a member of the three-member Advisory Committee, for his decisive contribution, his support, and of course his necessary "ophthalmological" look throughout the present research, to which he presented his own style. He contributed decisively to the acquisition of this unique and wonderful idea through his own creation. He has been a mentor to me and was the first to open the way for me and make me love the research process.

Many thanks to the excellent optometrists, Constantine Spelas and Ioannis Kormpakis for our amazing cooperation, their painstaking effort and their help.

I thank my parents who are always by my side in whatever I choose to support me with their undivided, selfless and infinite help and love. Finally, I would like to thank in particular a member of my family whose presence throughout the effort was decisive. My husband Angelos Trellopoulos has been for me the strength, the personification of the hope that I can do it and his own work is a model for my own goal.

This dissertation is dedicated to my family as a whole, but also to each of its members individually, who always supports me, lands me and takes me off. In a family that is always there for me.

CONTENTS

MEDICAL PART

OCULAR ANATOMY.....	7
1.1 The Orbit.....	7
1.2 The eyelids and the tear film.....	7
1.3 The globe.....	8
1.4 Conjunctiva.....	9
1.5 Cornea.....	10
1.6 Sclera.....	11
1.7 Uvea.....	12
1.8 Anterior and posterior chamber.....	14
1.9 Aqueous humor.....	14
1.10 Crystalline lens.....	15
1.11 Vitreous.....	16
1.12 Retina.....	16
1.13 Macula.....	18
1.14 The optic nerve.....	18
REFRACTIVE ERRORS.....	19
2.1 Basics of refractive errors.....	19
2.2 Prevalence of refractive errors.....	21
2.3 Myopia.....	21
2.4 Hyperopia.....	23
2.5 Astigmatism.....	23
2.6 Presbyopia.....	25
REFRACTIVE SURGERY.....	26
3.1 Basics of refractive surgery.....	26
3.2 Flap procedures.....	27
3.3 Surface procedures.....	29
3.4 Corneal incision procedures.....	31
3.5 Other procedures.....	33
CONTRAST SENSITIVITY.....	35
4.1 Basics of contrast sensitivity.....	35
4.2 Contrast Sensitivity Charts.....	37

4.2.1 Grating charts.....	37
4.2.2 Letter Charts.....	40
4.2.3 Computer Based Testing.....	42
<u>METHODS</u>	
LINEAR REGRESSION ANALYSIS	44
5.1 Background.....	44
5.2 Simple Linear equation	45
5.3 Linear regression equation	45
5.4 Multiple linear regression analysis.....	46
5.5 Assumptions	47
5.6 Checking for violations of model assumptions	47
5.7 Deviations from model assumptions	48
5.8 Goodness of fit.....	48
5.9 Selection methods for Linear Regression modeling	48
LINEAR MIXED MODELS ANALYSIS	48
6.1 Random Effects.....	49
<u>SPECIAL PART</u>	
SCOPE.....	49
INTRODUCTION.	50
MATERIALS AND METHODS.....	51
9.1 Study design and Population.....	51
9.2 Outcome Measurements and data collection.....	51
9.2.1 CS Assessment.....	52
9.2.2 SPARCS.....	52
STATISTICAL ANALYSIS	53
RESULTS	53
DISCUSSION	57
CONCLUSION	59
REFERENCES.....	60
ABSTACTS	69
APPENDICES	70

1. OCULAR ANATOMY

1.1 The orbit

The globe of the eye (*Figure 1.1.b*) is placed in a protective quadrilateral pyramid, bony socket in the skull, called the orbit (*Figure 1.1.a*). Seven bones conjoin to form the orbital structure. There is a very thin orbital floor (consisting of the maxillary, palatine, and zygomatic bones), a medial wall (consisting of the frontal process of the maxilla, lacrimal bone, orbital plate of the frontal bone, and lesser wing of the sphenoid), an orbital roof (consisting of the frontal bone), and a lateral wall (consisting of the zygomatic and greater wing of the sphenoid). The orbit, protects, supports, and maximizes the function of the eye. Moreover, the orbit contains and protects fat, blood vessels, the optic nerve, other nerves of the eye and six extraocular muscles that are attached to the eye and move it up and down, side to side, and rotate it. (Kaplan, 2007)

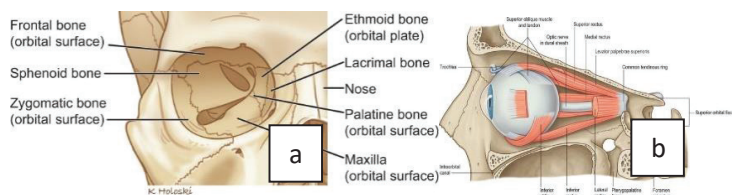


Figure 1.1 a. The orbit b. The glob

1.2 The eyelids and the tear film

The globe of the eye is also protected by the eyelids (*Figure 1.2.a*), whose surgical anatomy is one of the most complex in the head and neck. They act as a barrier to foreign bodies and lubricate the ocular surface. The upper and lower eyelids are comprised of skin, subcutaneous connective tissue, muscles (orbicularis oculi muscle the retractors, superior or inferior tarsal muscle), the tarsal plates, which consist of dense connective tissue and cartilage and the conjunctiva and glands.) The glands produce the tear film, which is about 7 μ m thick, covers the corneal epithelium by degreasing it, protects against injuries and infections and creates a smooth layer that helps light to penetrate the eye. It is the first layer of the cornea with which light comes into contact. It is a trilaminar layer consisting of an anterior lipid layer, a middle aqueous layer, and a posterior mucin layer. The anterior layer of the tear film (*Figure 1.2.b*) is secreted primarily by the meibomian glands that are oriented vertically in two parallel rows inside the

tarsal plate and retains the evaporation of the underlying water layer. The sebaceous glands of Moll and Zeis also secrete lipids. They are in the lid margin, in close relation to the eyelashes and keeps them supple. The middle aqueous layer is secreted by the main gland and the accessory lacrimal glands of Krause and Wolfring. The main lacrimal gland is located in a shallow depression within the orbital plate of the frontal bone, under the outside edge of the eyebrow. The accessory lacrimal glands Krause and Wolfring are located in the conjunctival fornices. Goblet cells which lie in the crypts of Henlé and the glands of Manz on the bulbar conjunctiva produces the posterior mucous layer, which retains the tear film in the cornea. Tear film is spread over the surface by periodic blinking. Then a pumping action is created with the contraction of the muscle, which facilitates drainage of fluid into the nasal cavity. This system comprises a single punctum at the medial aspect of each upper and lower tarsus, which is connected to a common canaliculus that drains into the lacrimal sac. The sac then drains in via the nasolacrimal duct and terminates intranasally through the valve of Hasner in the inferior meatus. (Kaplan, 2007; Sand, 2016; Sridhar, 2018)



Figure 1.2 a. The eyelids b. The tear film

1.3 The globe

The eyeball (*Figure 1.3*) is generally less tall than it is wide. The sagittal vertical (height) of a human adult eye is approximately 23.7 mm, the transverse horizontal diameter (width) is 24.2 mm and the axial anteroposterior size (depth) averages 22.0–24.8 mm with no significant difference between sexes and age groups. The typical adult eye has an anterior to posterior diameter of 24 millimetres, a volume of six cubic centimetres and a weight of 6.5 to 7.5 grams. (Bekerman, 2014; Cunningham 2011; Bron, 1997) The surface of the eye is also covered with conjunctiva. Its shape is spherical and has two poles, the anterior and the posterior. It consists of three layers, enclosing various anatomical structures and two cavities. The outer layer, known as the fibrous tunic, consists of the cornea (anterior 1/6) and the sclera (posterior 5/6), plays a protective role, provides shape to the eye and supports the deeper structures. The middle layer, known as the vascular tunic or uvea, consists of the choroid, ciliary body, pigmented

epithelium and iris and plays a nutritional role. The inner layer is the retina, which gets its oxygenation from the blood vessels of the choroid (posteriorly) as well as the retinal vessels (anteriorly). The anterior cavity is the anterior chamber between the cornea and the iris and through its angle, the aqueous humor is drained and the posterior chamber between the cornea and lens where the aqueous humor is produced by its radial body. The posterior cavity is the vitreous body, a jelly-like substance, behind the lens, filling the entire posterior cavity. (Oyster, 1999)

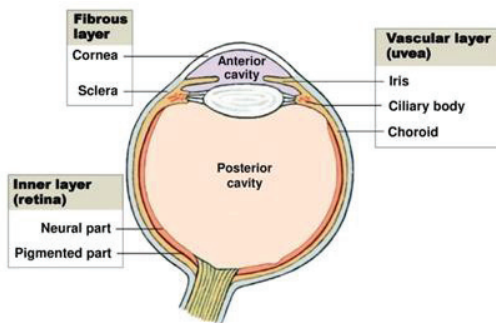


Figure 1.3 The eyeball

1.4 Conjunctiva

The conjunctiva (Figure 1.4) is a mucosal tissue made up of multilayered squamous epithelium, connective tissue and calyx cells (10%). It covers the posterior surface of the eyelids and the anterior part of the bulb up to the limbus. It contains small blood vessels that are visible to the naked eye. The conjunctiva helps lubricate the eye by producing mucus and tears, although a smaller volume of tears than the lacrimal gland. It also contributes to immune surveillance and helps to prevent the entrance of microbes into the eye. (Bron, 1997)

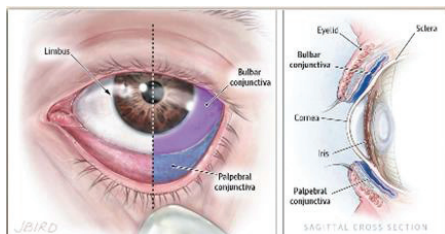


Figure 1.4 The conjunctiva

1.5 Cornea

Light is focused into the eye through the clear, dome-shaped front portion of the eye called the cornea (*Figure 1.5*). The cornea borders with the sclera via the corneal limbus. The cornea has unmyelinated nerve endings sensitive to touch causing an involuntary reflex to close the eyelid. Because transparency is of prime importance, the healthy cornea does not have or need blood vessels within it. Instead, oxygen dissolves in tears and nutrients are transported via diffusion from the tears, the aqueous humour and via neurotrophins supplied by the nerves of the cornea. (Nishida, 2010; Maggs, 2008) In humans, the cornea has a diameter of about 11–12 mm horizontally and 9–11 mm vertically and a central thickness to range from 551 to 565 μ and the peripheral thickness from 612 to 640 μ . The curvature of the anterior surface is on average 7.8 mm while that of the posterior 6.4 mm. (Kaufman, 1998) Its anterior surface is more curved in the central part and generally more curved than the sclera. Transparency, avascularity, the presence of immature resident immune cells, and immunologic privilege makes the cornea a very special tissue.

Its circumference gradually shifts to the sclera, overlapping, mainly up and down rather than to the sides, which is why its shape is elliptical. From a visual point of view, the cornea contributes most of the eye's focusing power (40-44 diopters) to collect light rays in the retina, accounting for approximately two-thirds of the eye's total optical power. (Goldstein, 2016; Fannin, 2013; Kaufman 1998; Sridhar, 2018))

Its structure consists, from the outside to the inside, of five layers. Recently, a layer of cornea which is well defined, acellular in pre-Descemet's cornea is getting attention with the development of lamellar surgeries. From the anterior to posterior the layers of the human cornea are:

Corneal epithelium: The epithelium (multilayered squamous) is a multicellular epithelial tissue layer that covers the surface of the cornea and is continuous with the conjunctival epithelium. Its thickness represents 10% of the thickness of the cornea, about 50 μ , and consists of 4-6 layers of cells which are shed constantly on the exposed layer and are regenerated by multiplication in the basal layer. It acts as a barrier to the penetration of microbes and pathogens and provides a smooth optical surface. (Ehlers, 1970)

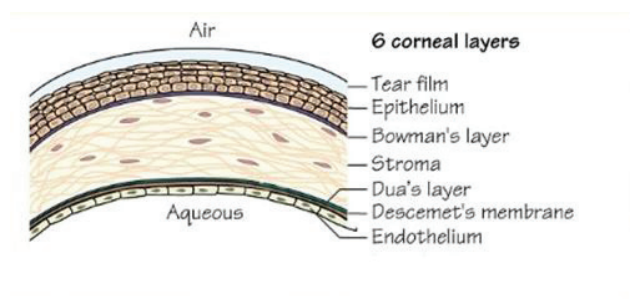


Figure 1.5 The cornea

The Bowman's membrane: The Bowman's membrane is just below the epithelium and is 8-12 μ thick. It is composed of collagen (mainly type I and V), laminin, nidogen, perlecan and other HSPGs. It is a very

durable surface that protects the corneal stroma and helps in maintaining the cornea shape, but does not regenerate after injuries.

Corneal stroma: The stroma constitutes about 80-85% of the cornea and is located under the Bowman's membrane. It consists of approximately 200 layers of collagen fibers arranged parallel to each other. This arrangement plays an important role in its clarity. There are scattered keratocytes, cells for general repair and maintenance, mainly between the layers. The predominant collagen is type I, but type III and IV coexist. It is the main refracting lens and gives mechanical strength to cornea. (Newsome, 1982)

Descemet's membrane: The Descemet's membrane is a thin cellular layer located below that serves as the modified basement membrane, secreted by the endothelium. It is composed mainly of collagen type IV fibrils, less rigid than collagen type I fibrils. It is about 5-10 μm thick, depending on the person's age.

Corneal endothelium: The endothelium consists of a layer of about 400,000 cells, 4-6 μm thick and is the most posterior surface of the cornea, which is moistened by the aqueous humor. It contributes to the nutrition of the cornea because it allows nutrients to pass through which contains the aqueous humor and regulates how much water should be concentrated in the cornea and maintains corneal clarity by removing water from the corneal stroma. Endothelial cells basically decrease after birth at an average of approximately 0.6% per year in normal corneas throughout adult life and do not regenerate. However, they show a remarkable ability to stretch and increase their size, in order to cover any gaps that are created after injury.

Dua's layer: Recently, a sixth layer of cornea has been described. It is a very thin and strong layer, anterior to Descemet's membrane, able to withstand 1.5 to 2 bars of pressure. (Dua, 2013)

1.6 Sclera

The sclera (*Figure 1.6*) is commonly known as the white part and is the outer and most durable, opaque, fibrous, protective layer of the eye on which the tendons of the oculomotor muscles resort. It forms the posterior five-sixths of the globe. It is thicker at the posterior pole (1 mm) and gradually thins forward, while its thinnest point is behind the rectus muscle attachment (0.3 mm). The sclera is perforated by many nerves and vessels passing through the posterior scleral foramen, the hole that is formed by the optic nerve. The sclera's blood vessels are mainly on the surface. In children, the sclera is thinner and more

transparent, giving it a bluish tinge due to the underlying choroid. The hardwood acquires a yellowish tinge with age. The sclera continuous with the dura mater and the cornea, and maintains the shape of the globe, offering resistance to internal and external forces, and provides an attachment for the extraocular muscle insertions. (Nishida,2010; Maggs, 2008)

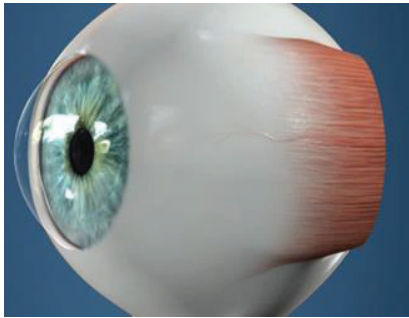


Figure 1.6 The sclera

1.7 Uvea

The uvea is the vascular layer of the eye and is located between the retina and the sclera. It consists of the iris, the ciliary body and the choroid. (Park, 1999)

Behind the anterior chamber is the eye's iris (the colored part of the eye) and the dark hole in the middle called the pupil. Muscles in the iris dilate (widen) or constrict (narrow) the pupil to control the amount of light reaching the back of the eye.

The iris (Figure 1.7) is a thin, annular structure, which separates the anterior from the posterior chamber and consists mainly of a vascular layer, melanocytes, nerves, collagen and mucosal polysaccharides. It is responsible for controlling the diameter and size of the pupil and thus the amount of light reaching the retina. It is stimulated by the anterior and long posterior radial arteries, which before joining the iris and form the major arterial cycle. The iris consists of two layers: the front pigmented fibrovascular layer known as a stroma and, beneath that, pigmented epithelial cells. The stroma is connected to the sphincter pupillae, which contracts the pupil in a circular motion, and a set of dilator muscles (dilator pupillae) which pull the iris radially to enlarge the pupil, pulling it in folds. The back surface is covered by a heavily pigmented epithelial layer that is two cells thick, but the front surface has no epithelium. The high pigment content defines the eye color and blocks light from passing through the iris to the retina, restricting it to the pupil. The outer edge of the iris, known as the root, is attached to the sclera and the anterior ciliary body. The iris and ciliary body together are known as the anterior uvea. Just in front of the

root of the iris is the region referred to as the trabecular meshwork, through which the aqueous humour constantly drains out of the eye, important structure for intraocular pressure.



Figure 1.7 The iris

The ciliary body (Figure 1.8) lies between the iris and the choroid. Its anterior portion, the pars plicata, forms about 70 radial projections that consist centrally of vessels surrounded by two epithelial stitches, which is the site of secretion of the aqueous humor. The middle part, the pars plana, 4 mm long is located between pars plicata and ora serrata. It is the surgical site of access to the posterior chamber in order to prevent injury of the lens or retina. The inner layer of pars plana consists of pigmented epithelial cells that continue backwards with the pigmented retinal epithelium. The outer layer consists of non-pigmented cells that secrete acidic polysaccharides, which are one of the main components of vitreous. The ciliary body consists of 3 degrees of smooth muscle tissue, the longitudinal, the radial and the circular, which are the ciliary muscle, which is innervated by the parasympathetic and when it contracts the zonule of Zinn and the lens of the eye relax becomes more convex in the ability to see closely.

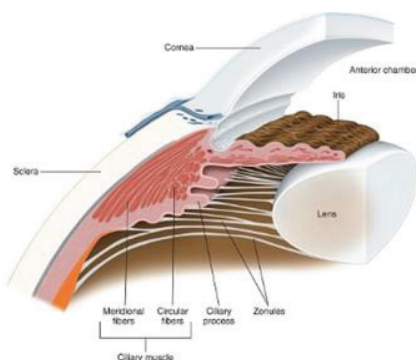


Figure 1.8 The ciliary body

The choroid (*Figure 1.9*) is the vascular layer of the eye, between the sclera and the retina, extends from the scleral spur anteriorly to the optic nerve posteriorly. It consists of blood vessels, melanocytes and connective tissue. It provides oxygen and nourishment to the outer retina, part of the optic nerve and the macula. Chorioid capillaries are a thin layer of capillaries located between the Bruch membrane and the retinal pigmented epithelium. They are the largest capillaries in the body with a diameter of 40-60 μm and contain multiple small openings and fenestrations through which small molecules can pass.

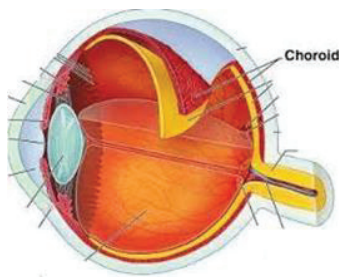


Figure 1.9 The choroid

1.8 Anterior and posterior chamber

The anterior chamber is the aqueous humor-filled space with a volume of 0.3 mL, is excised in front of the endothelium of the cornea and behind the iris and the anterior part of the lens. Its depth is about 3.4 mm, and it varies depending on the refraction, the ability to adapt, some endothelial diseases and age. The posterior chamber with a human volume of about 60-90 μL is excised in front of the posterior surface of the iris and the radial body behind the crystal lens and the fibers of the Zonule of Zinn. (Kaufman, 2003)

1.9 Aqueous humor

The aqueous humor (*Figure 1.10*) is produced and secreted by the epithelium of the ciliary body. The secretion of aqueous humor is active and passive. It is discharged mainly (90%) from the trabeculum that is located in the corner of the anterior chamber. The infiltrative portion is deposited in the Schlemm tube and eventually the aqueous humor accumulates and drains from the epidural veins. The remaining 10% is drained through the ragoid road, where the aqueous humor, through the ciliary body, is drained to the suprahorioid space. This procedure is important because if it is reduced or stopped, then the intraocular pressure increases resulting in the development of glaucoma. Normally there is a balance in the production and drainage of the aqueous humor, that is, the more it is produced, the more it is drained, with

the result the intraocular pressure being constant. The aqueous humor circulates in the anterior and posterior chambers, has a volume of approximately 0.3-0.4 mL, pH 7.38, moistens the lens, iris and cornea, and provides nutrients to these elements while maintaining and inflating the globe of the eye. It keeps the eyeball in a roughly spherical shape and keeps the walls of the eyeball taut. It also provides sodium, potassium, oxygen and glucose to the lens. In addition, it indicates a role in immune response to defend against pathogens.

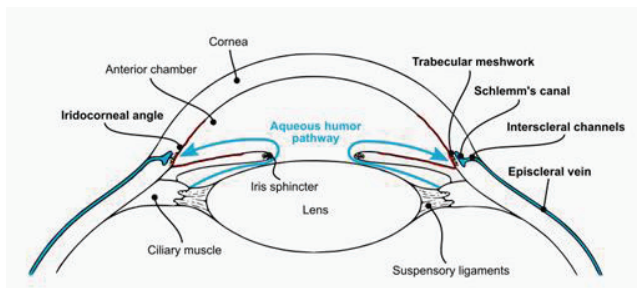


Figure 1.10 The Aqueous humor

1.10 Crystalline lens

The crystalline lens (*Figure 1.11*) is a transparent biconvex structure and is located behind the iris and in front of the vitreous. It weighs about 3 g, is about 16 ± 6 mm in diameter and has a maximum thickness of 3.95 ± 0.49 mm and is surrounded by a capsule. The lens content of proteins is over 30%. (Sakthivel, 2010) The predominant component of the lens is crystalline, which accounts for about 90% of all proteins. The composition of proteins and water changes over time (in old age), after injury or other causes resulting in loss of transparency (cataract). It acts as a refractory medium that focuses light on the retina. It has the ability to increase its anteroposterior thickness, acquiring a more spherical shape, thus changing its refractive power, which is estimated at about 25 diopters, one-third of the eye's total power. (Iribarren, 2012) Its elasticity allows the degree of curvature to fluctuate so that vision can be adjusted from distant to near objects almost instantly.

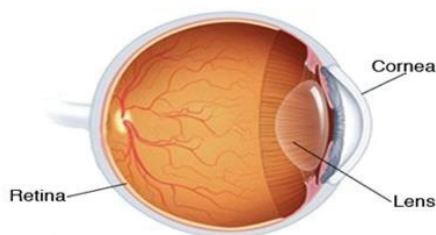


Figure 1.11 The crystalline lens

1.11 Vitreous

The vitreous (*Figure 1.12*) occupies 80% of the total ocular globe, with 4ml volume and 4gr weight, making it the largest anatomic structure in the human eye^{1, 2}. It is composed of 99% water and some type II and type IX collagen fibers, hyaluronic acid, fibrillin, opticin and mucopolysaccharides^{1, 3-5}. The vitreous is attached to different structures of the ocular fundus. The strongest attachment is at the vitreous base where the collagen fibers are particularly dense, with other attachments to the posterior lense, to the optic disc, to the macula and to the retinal vessels³⁻⁶. The vitreous is separated from the retina by the internal limiting membrane which encompasses type IV collagen³. It serves not only as a refractory medium but also to maintain the position and shape of the bulb as well as to support the lens. After the age of 50, the volume of the jelly decreases, while its liquefied volume increases. (Maher, 2012; Remington, 2011)

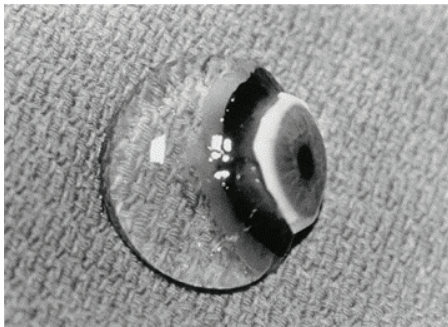


Figure 1.12 The vitreous

1.12 Retina

The retina (*Figure 1.13*) is a transparent layer, colorless and takes on a pinkish tinge from the choroid below. It is a light-sensitive tissue lining the back of the eye. It has a maximum thickness of 0.5 mm and contains millions of photoreceptors that sense light rays in a spectrum from 380 (violet) to 700 (Red) nanometers and convert them into electrical signals. The optics of the eye create a focused two-dimensional image of the visual world on the retina, which translates that image into electrical neural impulses which are sent to the brain to create visual perception. It consists of 10 anatomically separate layers, which from the outside to the inside are: 1) The retinal pigmented epithelium 2) The layer of photoreceptors (rods and cones) 3) The outer limiting membrane 4) The outer nuclear layer 5) The outer

plexiform layer 6) The inner nuclear layer 7) The inner plexiform layer 8) The ganglion cell layer 9) The nerve fiber layer 10) The inner limiting membrane. (Kolb, 1995; Stewart, 2017)

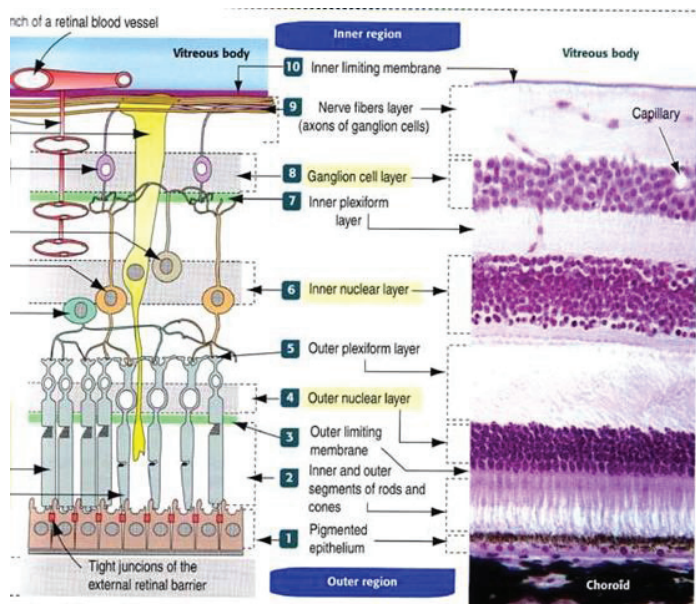


Figure 1.13 The retina

The pigmented epithelium (RPE) consists of a series of cuboidal epithelial cells and lies between Bruch's membrane and the outer sections of the photoreceptors. These cells contain a retinol-binding protein. It provides nourishment and supportive functions to the neural retina. The black pigment, melanin, in the pigment layer prevents light reflection throughout the globe of the eyeball, important for clear vision. The RPE also contributes to the formation of the external blood-retina barrier. (Thumann, 2001; Cunha-Vaz, 2011)

The photoreceptor layer consists of rods and cones. Rods function mainly in dim light, provide black-and-white vision, and are present away from the macula. Cones function in well-lit conditions, are responsible for the perception of color, as well as high-acuity vision used for tasks such as reading, and are concentrated in the macular area.

The outer limiting membrane is not exactly a membrane, but represents connections between MÜller cells and the inner parts of the photoreceptors.

The outer nuclear layer consists of eight to nine layers of photoreceptor cores.

The outer plexiform layer carries the synapses of the photoreceptors with the dendrites of bipolar cells and horizontal cells (synaptic cells).

The inner nuclear layer contains the nuclei of the amacrine cells, bipolar cells, and horizontal cells.[2] and Müller cells.

The inner plexiform layer consists mainly of synapses between the bipolar cell axons and the dendrites of the ganglion and amacrine cells

The ganglion cell layer consists of ganglion cells with a number ranging from 700,000 to 2 million.

The nerve fiber layer is made up of the axons of ganglion nerve cells.

The inner limiting membrane is the adhesion of the ends of the Muller cells to the surface of the nerve fibers.

1.13 Macula

The macula (*Figure 1.14*) is an oval-shaped, pigmented area near the center of the retina with a diameter of about 5.5 mm. It is both the thickest and in its center, the thinnest area of the retina, especially in its center, to allow direct light to fall on the optic cells. This area consists mainly of cones, has no rods and provides central vision, as it is the region of the retina where photoreceptors are most densely packed, it allows the highest resolution of images. The central 1.5 mm of the retina is bounded by the termination of the retinal capillary circulation. The 0.35 mm depression within the central macula, called the fovea by clinicians and the foveola by anatomists, has only cones in the photoreceptor layer. The terms parafovea and perifovea are often used in clinical practice to describe the locations of macular pathology. The macula is responsible for the central, high-resolution, color vision that is possible in good light. (Stewart, 2017)

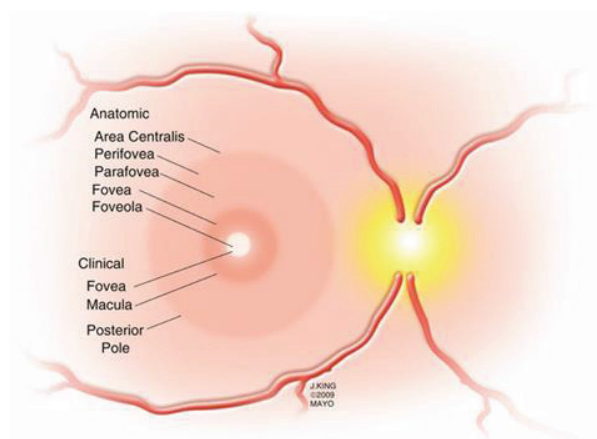


Figure 1.14 The macula

1.14 The optic nerve

The optic nerve (*Figure 1.15*), also known as cranial nerve II, transmits electrical pulses from the retina to the brain. It extends from the optic disc to the optic chiasma and continues as the optic tract to the lateral geniculate nucleus, pretectal nuclei, and superior colliculus. The optic nerve transmits all visual information including brightness perception, motion perception, color perception and contrast sensitivity. It also conducts the visual impulses that are responsible for two important neurological reflexes: the light reflex and the accommodation reflex. (Vilensky, 2015; Selhorst, 2009)

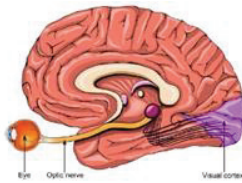


Figure 1.15 The optic nerve

2. REFRACTIVE ERRORS

2.1 Basics of refractive errors

The vision process relies heavily on the ability of the eye to refract light (*Figure 2.1*). The reflected light of the environment travels through the atmosphere and meets the first layer of the ocular system, the tear film. Afterwards, it enters through the crystal transparency of the cornea, the aqueous humor, the lens and the vitreous humor to project on the photoreceptors of the retina, whose impulses converge on the optic nerve and then to the brain. Continue adjustments to the pupil and lens regulate the entry and focusing of light.

The relaxed eye has an approximate optical power of 60 diopters (D). Most of the refractive power in the eye comes from the cornea, due to the differences in the indices of refraction. The corneal power is about 40 D, or two thirds of the total power and the lens is about 20 D, while in the fully accommodated state, it can temporarily increase to 33 D. The refractive index of the air is about $n \approx 1.00$, of the cornea $n \approx 1.3765$, of the aqueous humor $n \approx 1.3335$, of the crystalline lens $n = 1.40-1.42$ and of the vitreous humor $n \approx 1.335$. (Smith, 1997; Thompson, 2002; Pomerantzeff, 1984; Walsh, 1984)

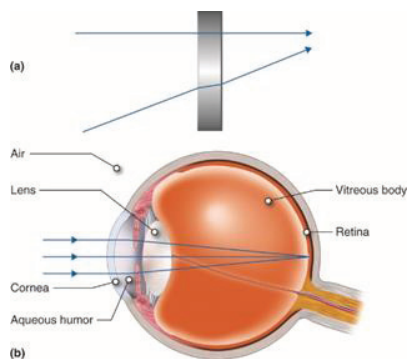


Figure 2.1 The ability of the eye to refract the light

Accommodation (Figure 2.2) involves the contraction and relaxation of the ciliary muscles to change the shape of the lens. The lens changes its shape in response to changes in tension of the ciliary muscles on the suspensory ligaments (also called zonules) that hold the lens in place. When the ciliary muscles contract, the suspensory ligaments are less taut, causing the lens to become slightly more spherical and refract light more. This is what happens when objects that are being viewed are close, or moved closer. Light coming from objects that are far away do not require as much refraction and are viewed with the ciliary muscles relaxed and more tension on the lens, which makes it more oblong. The relationship between the ciliary muscles and the tautness of the suspensory ligaments is a counterintuitive one for most individuals, but the eye has a unique anatomy that leads to this relationship.

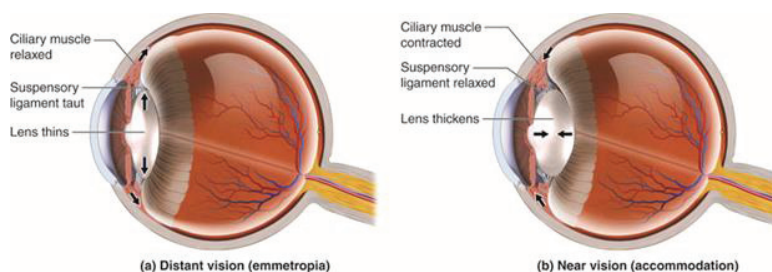


Figure 2.2 The accommodation

Along with accommodation of the lens when objects are near, the pupil also tends to constrict to allow less peripheral light to enter the posterior chamber of the eye. In doing so, objects can be viewed more crisply. The pupil will also constrict when conditions are bright and dilate under low light conditions. This way the retina can receive an appropriate amount of light to activate its photoreceptors without bleaching them with too much light.

In the normal eye, the image of an object is formed on the retina. This ideal refractive condition is called emmetropia and is generally rare. A refractive error (ametropia) is defined as failure of parallel light rays

to focus on the retina with the eye in a non-accommodating state. It is measured in diopters (D) and is classified as axially symmetrical, astigmatic, or (most commonly) mixed. Three conditions of ametropia are found, the axially symmetrical types of refractive error, nearsightedness (myopia) and farsightedness (hyperopia), and astigmatism. Although not adhering to the true definition of ametropia, presbyopia (agerelated inadequacy of accommodation) is often included.

2.2 Prevalence of refractive errors

It is estimated that globally 153 million people over 5 years of age are visually impaired as a result of uncorrected refractive errors, of whom 8 million are blind. There is no evidence of visual impairment caused by uncorrected refractive errors in children aged less than 5 years.

From the data reported in surveys it was not possible to distinguish conclusively between the prevalence of male and female cases of uncorrected refractive errors for any of the age groups.

Some 12.8 million in the age group 5–15 years are visually impaired from uncorrected or inadequately corrected refractive errors, a global prevalence of 0.96%, with the highest prevalence reported in urban and highly developed urban areas in south-east Asia and in China.

The number of people aged 16–39 years visually impaired from uncorrected refractive errors is 27 million, a prevalence of 1.1% globally. This could, however, be an underestimate, being derived directly from the prevalence in the age group 5–15 years, although the prevalence of refractive errors, especially myopia, is higher between the ages of 13 and 18 years.

The prevalence in people aged 40–49 years globally is 2.45%; it is high in subregions or countries where the prevalence for people aged 50 years and older is also high. Almost 95 million people aged 50 years and older are visually impaired from uncorrected refractive errors: the prevalence is between 2% and 5% in most regions of the world, but is almost 10% in China and almost 20% in India and in Sear-D.

Of the 95 million people aged 50 years and older visually impaired from uncorrected refractive errors, 6.9 million are blind. Based on this, it is estimated that 1.3 million people in the age group 40–49 years are blind from uncorrected refractive errors. There was no evidence in any surveys of significant blindness in the age groups 5–15 years and 16–39 years. (WHO, 2006)

2.3 Myopia

Myopia (*Figure 2.3*) is the most common eye problem and is estimated to affect 1.5 billion people (22% of the population). Myopia, or near sightedness, is present when the eye is too long in relation to its refractive apparatus, so the focal plane of light entering the eye is anterior to the retina and leads to poor

visual acuity for distant objects but improved visual acuity for close objects. The farther this point is, the duller the image formed in the retina. Blurring of distance vision is universal and proportionate to the degree of myopia. Patients with lower degrees of myopia have the advantage of clear near vision, as the divergent rays from the near object come to focus on the retina with no need for accommodative effort or need for correction. (Foster, 2014; Holden, 2014)

This refractive error of the eye is divided into two categories, the refractive and the axial myopia.

Refractive myopia occurs when the refractive power of the lens system is too strong for the axial length of the eye. Parameters of the lens system are the curvature of the cornea, the curvature of the lens at the front as well as at the back, and the refractive indices of the anterior chamber, the lens and the vitreous body.

Axial myopia occurs when the distance between the lens system and the retina (axial length) is too long for the optical power of the eye. There are several forms of axial myopia:

Simple myopia, which normally starts at age 10-12, stays normally under -6D and remains quite stable after the age of 20 years. No structural defects of the eye can be diagnosed in this case.

Benign progressive myopia up to 12 D, which is often stabilized at an age of 30 years. Most likely structural/ biochemical defects of the eye can be diagnosed.

Malign myopia, which does not stop progressing at all. Up to -30 D can be reached, with serious consequences, which may lead to blindness.

Pathological myopia, if there are already pathological changes in the eye, independent from the refractive error, such as vitreous liquefaction and detachment, retinal detachment, various myopic maculopathies, choroidal neovascularization, posterior staphyloma, glaucoma.

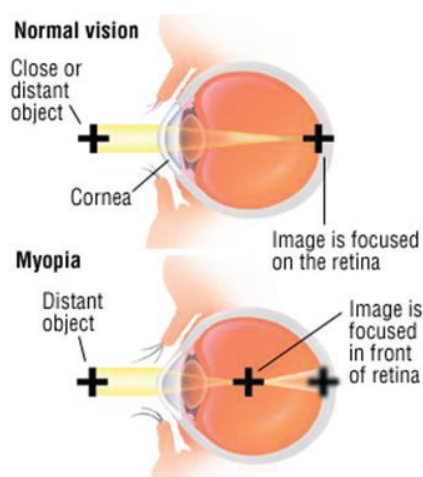


Figure 2.3 Myopia

2.4 Hyperopia

Hyperopia (*Figure 2.4*), or far sightedness, is the condition, in which the focal plane of light entering the eye is posterior to the retina and leads to poor visual acuity for close objects but improved visual acuity for distant objects. The optical power of the eye in the case of hyperopia is less than it should be and the axial length is shorter than normal (the commonest cause). A combination of several factors often co-exist. In younger age, much of the hyperopia can usually be corrected by the patient's own accommodation, which increases the effective power of the eye bringing incident rays to a focus on the retinal level (facultative hyperopia). With advancing age the accommodative effort cannot be sustained and symptoms of hyperopia with blurring, headaches and eyestrain become more and more manifest. People may also experience accommodative dysfunction, binocular dysfunction, amblyopia, and strabismus. In addition, they have an increased risk of angle closure glaucoma and early onset of presbyopia. (Lowth, 2016; Moora, 2008)

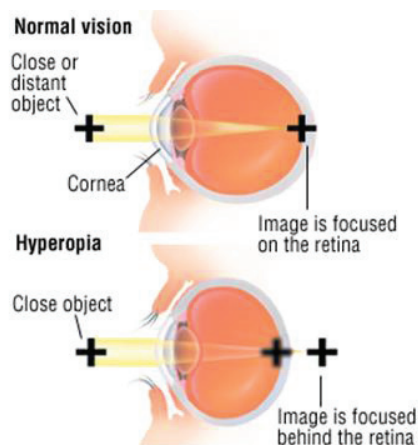


Figure 2.4 Hyperopia

2.5 Astigmatism

Astigmatism (*Figure 2.5*) arises when one or both of the two refractive media – the cornea and the lens – has a different curvature, and therefore a different refractive power, in two meridians. The cornea surface has an ellipsoid schema. If this ellipsoid is cut into two sectors perpendicular to each other, these two sectors are the two main meridians, to which the smallest and largest optical powers, respectively, correspond. When this is the case, the uneven refraction of a light ray that is incident upon the eye results

in the projection of a displaced or distorted image onto the retina, rather than a point image. The different visual power along the two meridians causes the so-called astigmatism. (Gilbert, 2005)

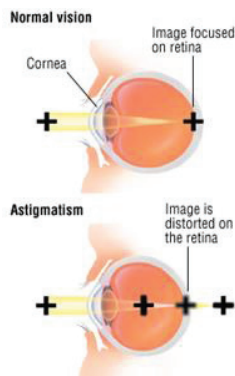


Figure 2.5 Astigmatism

Astigmatism is distinguished into symmetrical where the meridians are perpendicular to each other (90 degree angle), and asymmetric where the meridians form an angle different from 90 degrees. The asymmetry can only be detected by keratometry or topography. Astigmatism is referred to as a cylinder (difference in optical power between the two main meridians) and as an axis (direction in which the abstraction is shorter, and the image clearer) is expressed in degrees from 1 to 180. Astigmatism is always refractive because it is not possible the eye to have different lengths in two meridians. A common phenomenon is that astigmatism is due either to the cornea, so we are talking about corneal astigmatism, or asymmetry of the crystalline lens, or non-eccentric placement of refractive elements in the optical axis. If the vertical meridian has a smaller radius of curvature than the horizontal we have astigmatism with the rule, while if it is flatter we have the astigmatism against the rule.

Astigmatism does not form a point or a focus inside (or outside) the eye, but two focal lines that are farther apart the greater the astigmatism (Sturm's conoid) (Figure 2.6). Between them (in power diopters and not in distance) is formed the cycle of minimal confusion, in which the image has the best sharpness.

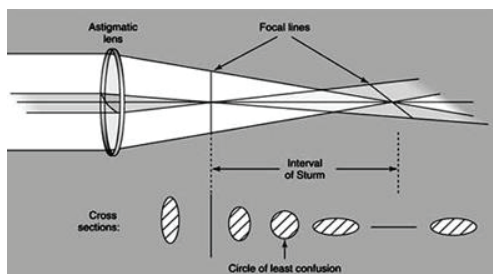


Figure 2.6 Sturm's conoid

Depending on the axis of the principal meridian, astigmatism is divided into five types:

Regular astigmatism where principal meridians are perpendicular.

With-the-rule astigmatism where the vertical meridian is steepest

Against-the-rule astigmatism where the horizontal meridian is steepest

Oblique astigmatism where the steepest curve lies in between 120 and 150 degrees and 30 and 60 degrees.

Irregular astigmatism where principal meridians are not perpendicular.

Depending on the focus of the principal meridian, astigmatism is divided into five types:

Simple myopic: where one focal line is on the retina and the other in front of it

Compound myopic: where the two focal lines are in front of the retina

Simple hyperopic: where one focal line is on the retina and the other behind it

Compound Hyperopic: where the two focal lines are behind the retina

Mixed: where one focal line is in front of the retina and the other behind it.

2.6 Presbyopia

The word presbyopia (*Figure 2.7*) is based on a Greek word that means "aging eye". With growing age, the amplitude of true accommodation decreases, beginning early in life-in childhood or adolescence. The optical power of the eye is 60 D so as to form a sharp retinal image of a distant object located from 6m and up. The cornea contributes to the formation of this image, as it is responsible for 2/3 of the refractive power required to observe the object. When we read and write the object is at a distance of 25-50cm. At these distances the normal optical power of 60 D is not enough. In order to achieve good visual acuity for objects that are closer to the eye, the lens increases its visual power with a process called accommodation. During the accommodation, the curvature of the lens increases and comes a little further towards the iris, and as a result its refractive power increases and it focuses the image of the object on the retina. Over time, there is a gradual decrease in accommodation, because the crystalline lens loses its flexibility because it hardens in texture by decreasing levels of α -crystallin, a process which may be sped up by higher temperatures (Pathai, 2013), and the strength and elasticity of the ciliary muscle is lost, as well as the zonular fibers. This condition is known as presbyopia. Symptoms include discomfort of near vision, difficulty reading small print, having to hold reading material farther away, headaches, and eyestrain. Typically, between the ages of 38 and 43 years, these changes reach the stage at which accommodative loss is sufficient to cause the blurred-vision symptoms of presbyopia. In reality the ability to focus on near objects declines throughout life, from an accommodation of about 20 dioptres (ability to focus at 50 mm away) in a child, to 10 dioptres at age 25 (100 mm), and levels off at 0.5 to 1 dioptre at age 60 (ability to

focus down to 1–2 meters only). Hyperopic people know the symptoms of presbyopia earlier and myopics later. (Robert, 1998)

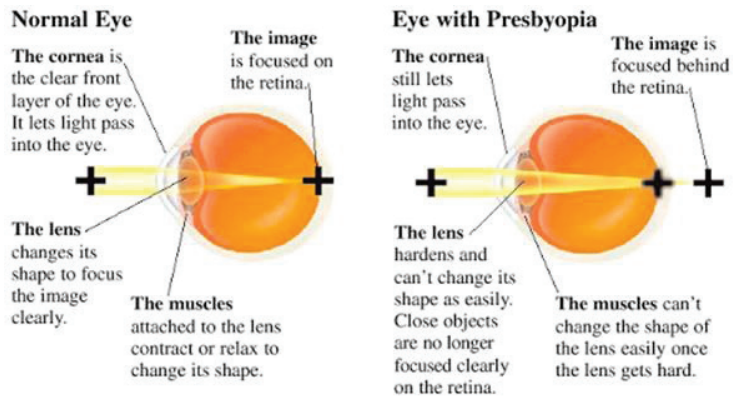


Figure 2.7 Presbyopia

3. REFRACTIVE SURGERY

3.1 Basics of refractive surgery

Refractive surgery, a subfield of ophthalmology, is defined as the surgical correction of refractive errors of the human eye. The first theoretical work on the potential of refractive surgery was published in 1885 by Hjalmar August Schiøtz, an ophthalmologist from Norway. (Schiøtz, 1885) The goal of refractive eye surgery is to improve the refractive state of the eye and to decrease or eliminate dependency on eyeglasses or contact lenses. It has become a highly specialized area in the last few years. Ophthalmic surgeons now have a multiplicity of refractive surgical methods at their disposal for the individualized correction of refractive errors. Techniques of refractive surgery on the cornea and lens are now available that meet standard criteria of safety, efficacy, cost-effectiveness, and predictability of the refractive outcome. This can include various methods of surgical remodeling of the cornea (keratomileusis; corneal reshaping (from Greek *kéras*: horn and *smileusis*: carving)), lens implantation or lens replacement. The most common methods today use excimer lasers to reshape the curvature of the cornea. An excimer ("excited dimer") laser is an argon fluoride laser operating with a wavelength of 193 nanometers. The cornea is remodeled with laser ablation intended to cause light rays falling upon the eye join together on the macula). (Li,2017)

Types of surgery to correct refractive errors include:

3.2 Flap procedures

Excimer laser ablation is done under a partial-thickness lamellar corneal flap.

Automated lamellar keratoplasty (ALK (Figure 3.1)): This is used for hyperopia and severe cases of myopia. For myopia, the eye surgeon cuts a flap across the front of the cornea with a special tool (microkeratome). The flap is folded to the side. A thin slice of tissue is removed from the surface of the cornea. This flattens the central cornea and reduces refraction. The flap is then put back in place. The flap reattaches itself without stitches. During ALK for hyperopia, the eye surgeon makes a deeper cut into the cornea with the microkeratome to make a flap. The pressure in the eye causes the corneal surface to stretch and bulge. The bulging cornea improves the optical power. This is intended to correct the hyperopia. The flap is then put back in place. It reattaches without stitches. Possible complications of ALK surgery include overcorrected or undercorrected vision, astigmatism, inability to wear contact lenses, loss of the corneal flap and need for a corneal graft, scarring, infection, vision loss and glare.

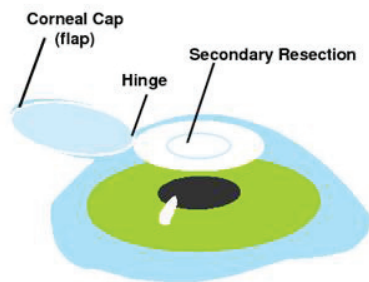


Figure 3.1 Automated Lamellar Keratoplasty

Laser-assisted in situ Keratomileusis (LASIK (Figure 3.2)): The name LASIK was coined in 1991 by University of Crete and the Vardinoyannion Eye. (TO VIMA, 2009) This is surgery to correct myopia, hyperopia, or astigmatism. The procedure reshapes the cornea with an excimer laser. LASIK has replaced many of the other refractive eye surgery methods. This surgery is done using a computer-controlled excimer “cold” laser. It also uses a tool called a microkeratome (femtosecond laser). With these tools, the surgeon cuts a flap in the center of the cornea. A thin layer of tissue is ablated in a deeper layer of the cornea, i.e., the anterior stroma. After ablation, the flap is put back into its original position, where it sticks to the cornea without any further intervention because of adhesive forces and the pumping effect of the endothelium, and then becomes definitively fixed in place by tissue growth within a few hours. Modern aspheric (i.e., deviating from spherical shape) and wavefront-guided ablation profiles are used to prevent the generation of higher-order aberrations (HOA) of the eye, or to reduce HOA that are already present, and thus improve the patient's vision. To adjust the ablation profile more precisely, "eye trackers"

registering the position of the iris are used to correct for horizontal, vertical, and rotatory eye movements. An eye tracker is a pursuit system that ensures the removal of corneal tissue at the intended location and prevents accidental decentering of the ablation zone. It can compensate for ocular saccades that occur during treatment. This can give sharper vision and reduce nighttime vision problems. (Azar, 2007; Solomon, 2009))

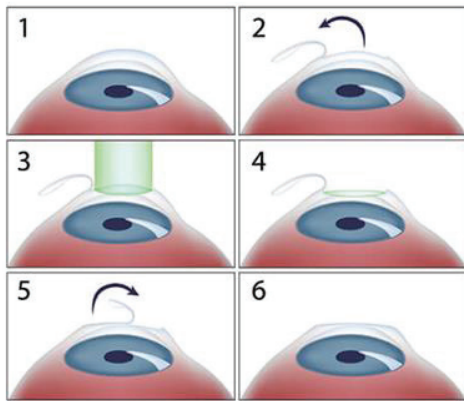


Figure 3.2 Laser in Situ Keratomileusis

Refractive Lenticule Extraction (ReLEx):

ReLEx "FLEx" (Femtosecond Lenticule Extraction (Figure 3.3)): A femtosecond laser cuts a lenticule within the corneal stroma. Afterwards, a LASIK-like flap is cut which can be lifted to access the lenticule. This is removed through manual dissection using a blunt spatula and forceps. The femtosecond laser is the newest technology for creating a corneal flap risk of a cutting error, as may occur with a mechanical microkeratome, is low. The 40- and 50-kHz lasers that were previously used have now been replaced by 60-kHz lasers, which are currently available on the market. This technology also prevents the occurrence of delayed hypersensitivity syndrome (DHS). The time needed for visual rehabilitation is roughly the same whether the corneal flap is created with femtosecond laser or with a microkeratome. Despite their advantages, femtosecond lasers are used in only a few centers at present.

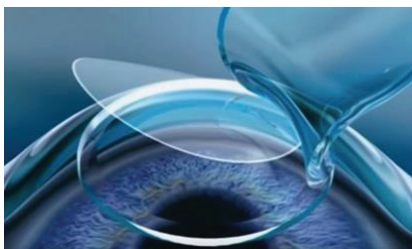


Figure 3.3 Femtosecond Lenticule Extraction

ReLEx "SMILE" (Small Incision Lenticule Extraction (*Figure 3.4*)): A newer technique without a flap, a femtosecond laser cuts a lenticule within the corneal stroma. The same laser is used to cut a small incision along the periphery of the lenticule about 1/5th the length of a standard LASIK flap incision. The surgeon then uses a specially designed instrument to separate and remove the lenticule through the incision, leaving the anterior lamellae of the cornea intact. No excimer laser is used in the "ReLEx-procedures". (Li, 2017)

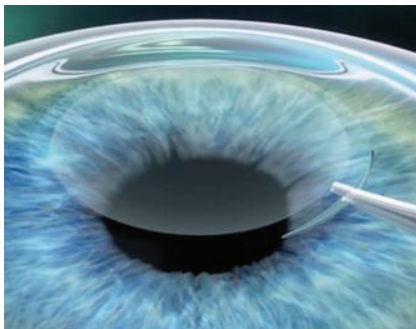


Figure 3.4 Small Incision Lenticule Extraction

3.3 Surface procedures

The excimer laser is used to ablate the most anterior portion of the corneal stroma. These procedures do not require a partial thickness cut into the stroma. Surface ablation methods differ only in the way the epithelial layer is handled. (Amar, 2009)

Photorefractive keratectomy (PRK (Figure 3.5)) is an outpatient procedure generally performed with local anesthetic eye drops (as with LASIK/LASEK). It is a type of refractive surgery which reshapes the cornea by ablating microscopic amounts of tissue from the outer surface of the corneal stroma, using a computer-controlled beam of light to map the eye's surface and to calculate how much tissue to ablate (excimer laser). The difference from LASIK is that the corneal epithelium is removed (and a bandage contact lens is used); no flap is created. Recovery time is longer with PRK than with LASIK, though the final outcome (after 3 months) is about the same. This surgery is done with the same kind of excimer laser used for LASIK. PRK is done to reshape the cornea to correct mild to moderate nearsightedness (myopia). Because the cornea surface is removed, it takes a few weeks to heal. (Amar, 2009)

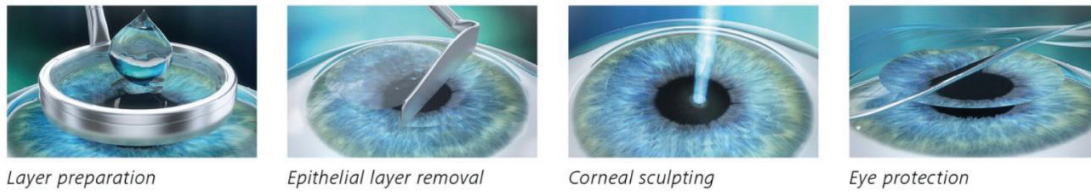


Figure 3.5 Photorefractive Keratectomy

Transepithelial photorefractive keratectomy (TransPRK (Figure 3.6)) is a laser-assisted eye surgery to correct refraction errors of human eye cornea. It employs excimer laser to ablate outer layer of cornea, epithelium, as well its connective tissue, stroma, to correct eye optical power.

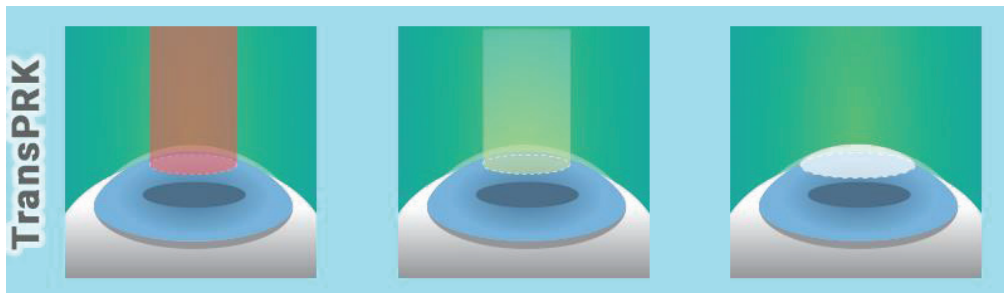


Figure 3.6 Transepithelial photorefractive keratectomy

Laser Assisted Sub-Epithelium Keratomileusis (LASEK (Figure 3.7)) is a procedure that also changes the shape of the cornea using an excimer laser to ablate the tissue from the corneal stroma, under the corneal epithelium, which is kept mostly intact to act as a natural bandage. The surgeon uses an alcohol solution to loosen then lift a thin layer of the epithelium with a trephine blade (usually with a thickness of 50 micrometres). During the weeks following LASEK, the epithelium heals, leaving no permanent flap in the cornea. This healing process can involve discomfort comparable to that with PRK.

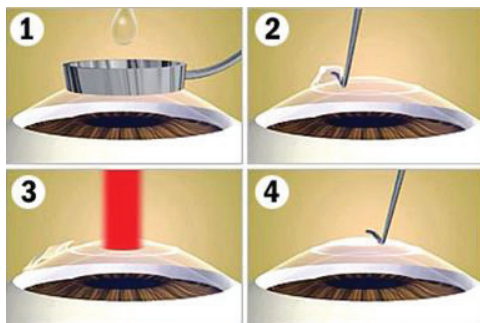


Figure 3.7 Laser Assisted Sub-Epithelium Keratomileusis

EPI-LASIK (Figure 3.8) is a new technique similar to LASEK that uses an epi-keratome (rather than a trephine blade and alcohol), to remove the top layer of the epithelium (usually with thickness of 50 micrometres), which is subsequently replaced. For some people it can provide better results than regular LASEK in that it avoids the possibility of negative effects from the alcohol, and recovery may involve less discomfort.

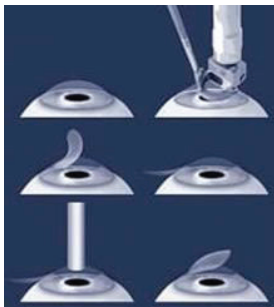


Figure 3.8 EPI-LASIK

Customized Transepithelial No-touch (C-TEN (Figure 3.9)) is an innovative strategy for corneal surgery that avoids any corneal manipulation via a complete laser-assisted trans-epithelial approach. Since C-TEN is planned on the morphology of each individual eye, it can treat a large variety of corneal pathologies from refractive to therapeutic. C-TEN is sometimes referred to as Advanced Surface Ablation (ASA). (Isaak, 2010)

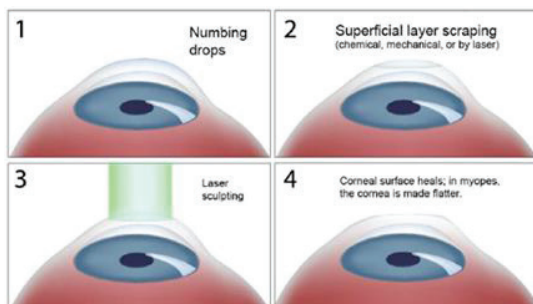


Figure 3.9 Customized Transepithelial No-touch

3.4 Corneal incision procedures

Radial keratotomy (RK (Figure 3.10)), developed by Russian ophthalmologist Svyatoslav Fyodorov in 1974. This technique is, in medium to high diopters, usually replaced by other refractive methods. Tiny

cuts (incisions) are made in the cornea with a diamond scalpel. The cuts cause flatten the center of the cornea and change its curve. This reduces refraction. Because the cornea is cut, it takes a few weeks to heal. This surgery was very common. But it has been nearly replaced by LASIK.

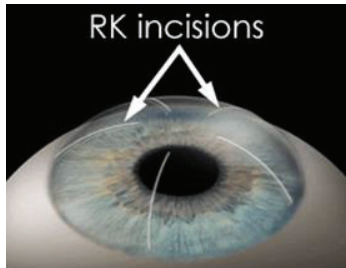


Figure 3.10 Radial keratotomy

Arcuate keratotomy (AK (Figure 3.11)), also known as Astigmatic keratotomy, uses curvilinear incisions at the periphery of the cornea to correct high levels of non-pathological astigmatism, up to 13 diopters. A diamond knife or femtosecond laser is used to make multiple microscopic cuts perpendicular to the steep meridian of the cornea in order to alter the corneal surface curvature. AK is often used for the correction of high post-keratoplasty astigmatism or post-cataract surgery astigmatism. Astigmatic keratotomy (AK) is similar to radial keratotomy (RK).

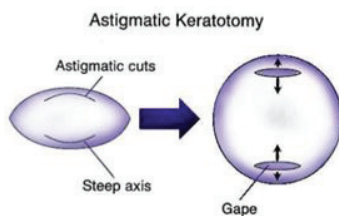


Figure 3.11 Arcuate keratotomy

Limbal relaxing incisions (LRI (Figure 3.12)) are incisions near the limbus (outer edge of the iris), used to correct minor astigmatism (typically less than 2 diopters). This is often performed in conjunction with an Intraocular Lens implantation.



Figure 3.12 Limbal relaxing incisions

3.5 Other procedures

Radial Keratocoagulation (Figure 3.13), also known as Radial Thermokeratoplasty, was invented in 1985 by Svyatoslav Fyodorov and is used to correct hyperopia by putting a ring of 8 or 16 small burns surrounding the pupil, intended to steepen the cornea as a result of constriction of the burned tissue; It can also be used to treat selected types of astigmatism. It is now generally replaced by laser thermal keratoplasty/laser thermokeratoplasty.



Figure 3.13 Radial Keratocoagulation

Laser thermal keratoplasty (LTK (Figure 3.14)) is a non-touch thermal keratoplasty performed with a Holmium laser, while conductive keratoplasty (CK) is thermal keratoplasty which is used to correct mild to moderate hyperopia. It uses heat from low-level radio waves to shrink the collagen and change the cornea's shape. A probe smaller than a strand of hair is used to apply the radio waves around the outer cornea. This creates a tight band. The band increases the curve of the cornea and is intended to improve vision. The procedure is limited to those 40 years of age or older.



Figure 3.14 Laser thermal keratoplasty

Intrastromal corneal ring segments (Intacs (Figure 3.15)) are approved by FDA for treatment of low degrees of myopia. These are used to treat mild myopia. They are thin rings that are implanted into the cornea, intended to change the curve of the cornea and improve vision.

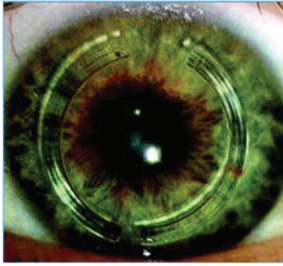


Figure 3.15 Intrastromal corneal ring segments

Refractive lens surgery: An artificial lens (intraocular lens) can be implanted into the eye either in addition to, or instead of, the natural lens: phakic intraocular lenses (PIOL) are implanted into the eye without removing the natural lens, while the lens is removed when a refractive lens exchange (RLE) is performed. These methods leave the cornea untouched and are particularly advantageous for patients with high refractive errors and corneal pathology. However, they introduce the serious risks related to all intraocular surgical procedures. (Amar, 2009)

Phakic intraocular lenses (Figure 3.16) are implanted into the human eye in addition to the natural ocular lens. They can be implanted into either the anterior or the posterior chamber. Anterior chamber lenses come in two kinds – angle-supported and iris-fixated – depending on the site where their position in the eye is secured. Posterior chamber lenses are implanted between the iris and the natural lens of the eye. Rigid PIOLs are made of polymethylmethacrylate (PMMA); there are also flexible ones made of acrylate and silicone that can be implanted through an 3 mm incision. Flexible PIOL are relatively easy to implant, and are also nearly astigmatism neutral. (Amar, 2009)



Figure 3.16 Phakic intraocular lenses

Refractive lens exchange (RLE) (Figure 3.17) is the replacement of the patient's natural ocular lens with an artificial one. The eye is opened at the edge of the cornea and the natural lens is broken down and suctioned away with the aid of an ultrasonic device, as in modern cataract surgery. A new, artificial lens is then inserted into the capsular bag: it may be either monofocal (i.e., suitable for sharp vision either at

close range or at a distance) or multifocal. Multifocal IOL have the advantage that the patient can see both near and far objects, without having to wear reading glasses for near vision. They have the disadvantages of increased cost, and decreased contrast sensitivity. (Amar, 2009)

Although the risk of complications is decreasing compared to the early days of refractive surgery, there is still a small chance for serious problems. These include vision problems such as ghosting, halos, starbursts, double-vision, dry-eye syndrome, overcorrected or undercorrected vision, irregular astigmatism, corneal haze or glare, sensitivity to light, inability to wear contact lenses, loss of the corneal flap and need for a corneal graft, scarring, infection, blurry vision or vision loss, infection, discomfort, cataract.

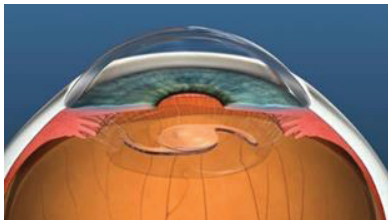


Figure 3.17 Refractive lens exchange

4. CONTRAST SENSITIVITY

Contrast sensitivity is an important aspect of visual function. The human visual system is more sensitive to contrast than absolute luminance; we can perceive the world similarly regardless of the huge changes in illumination over the day or from place to place. The ability to distinguish contrast plays an important role in patients' everyday vision. Patients may have 20/20 acuity and yet complain of poor vision if their contrast sensitivity is diminished. Contrast sensitivity testing can identify many ocular diseases. It plays a role in many aspects of vision, specifically motion detection, visual field, pattern recognition, dark adaptation, and visual acuity. It affects what patients can do in their daily life. Testing the peak of contrast sensitivity function provides a useful clinical adjunct to standard visual acuity assessments. This chapter reviews the basics of contrast sensitivity. It also describes the currently available contrast sensitivity tests and compares their reliability, advantages, and disadvantages. (Richman, 2013)

4.1 Basics of contrast sensitivity

Contrast is the difference in luminance or color that makes an object (or its representation in an image or display) distinguishable. In visual perception of the real world, contrast is determined by the difference in the color and brightness of the object and other objects within the same field of view. For example, a

black bird against white clouds has high contrast whereas a green bird against a green tree has low contrast. Contrast threshold is the smallest difference in lightness and darkness between an object and its background that can be distinguished. Contrast threshold is typically reported as contrast sensitivity, which is the inverse of the contrast threshold. Contrast sensitivity is often expressed in log units to make the values linear and allow comparison at low and high levels of contrast. There are many possible definitions of contrast. Some include color; others do not. Various definitions of contrast are used in different situations. Here, luminance contrast is used as an example, but the formulas can also be applied to other physical quantities. In many cases, the definitions of contrast represent a ratio of the type **“Luminance difference”/ “Average Luminance”**

The rationale behind this is that a small difference is negligible if the average luminance is high, while the same small difference matters if the average luminance is low (see Weber–Fechner law). Below, some common definitions are given. (Richman, 2013)

Weber contrast is defined as $(I - I_b)/I_b$ with **I** and **I_b** representing the luminance of the features and the background, respectively. The measure is also referred to as Weber fraction, since it is the term that is constant in Weber's Law. Weber contrast is commonly used in cases where small features are present on a large uniform background, i.e., where the average luminance is approximately equal to the background luminance.

Michelson contrast (also known as the visibility) is commonly used for patterns where both bright and dark features are equivalent and take up similar fractions of the area (e.g. sine-wave gratings). The Michelson contrast is defined as

$(I_{max} - I_{min}) / (I_{max} + I_{min})$ with **I_{max}** and **I_{min}** representing the highest and lowest luminance. The denominator represents twice the average of the maximum and minimum luminances. (Michelson, 1927; Lawrence, 2018)

This form of contrast is an effective way to quantify contrast for periodic functions $f(x)$ and is also known as the modulation m_f of a periodic signal f . Modulation quantifies the relative amount by which the amplitude (or difference) $(f_{max} - f_{min})/2$ of f stands out from the average value (or background) $(f_{max} + f_{min})/2$. In general, m_f refers to the contrast of the periodic signal f relative to its average value. If $m_f = 0$, then f has no contrast. If two periodic functions f and g have the same average value, then f has more contrast than g if $m_f > m_g$. (Prince, 2006)

Root mean square (RMS) contrast does not depend on the angular frequency content or the spatial distribution of contrast in the image. RMS contrast is defined as the standard deviation of the pixel intensities. (Peli, 1990)

The size of an object influences how much contrast is needed to differentiate the object from its background. Any object size can be depicted by lines of appropriate spacing occupying a specific visual angle. The number of adjacent dark and light lines (cycles) within a defined visual angle is called the spatial frequency. A high spatial frequency (higher number of cycles per degree [cpd]) is displayed as densely packed lines; a low spatial frequency is displayed as sparsely packed lines. The contrast sensitivity function represents the relationship between contrast sensitivity and spatial frequency.

4.2 Contrast Sensitivity Charts

Current contrast sensitivity charts commonly use gratings or letters at varying levels of contrast to determine patients' foveal contrast thresholds. The cycles per degree of the gratings or the size of the letters determine the spatial frequency being evaluated. The letter contrast charts are easily used and are familiar to those who perform and have ophthalmic examinations. Shortcomings of the letter charts include letters having different contrast thresholds and patients' varying levels of language ability. Patients unfamiliar with the Roman alphabet cannot be assessed with many standard letter charts. Some patients may have a high level (or low level) of ability to recognize reduced cues and therefore correctly (or incorrectly) guess at the correct letter. Both the gratings and letter charts are performed under standardized lighting, which is difficult to control among testing room environments. Moreover, charts can be affected by uneven lighting, reflections, fading, learning, and poor testing methods. (Richman, 2013)

4.2.1 Grating Charts

The Arden plates (Figure 4.1) were one of the first commonly used contrast sensitivity tests. Seven spatial frequencies are evaluated using sine wave gratings on 7 plates; contrast varies from the top to the bottom of each plate. Examiners slowly uncover a plate, and patients report when they first see the contrast bars. Weaknesses of the test design are that it is not forced-choice method and the results vary depending on the speed of exposing the contrast images. (Richman, 2013)

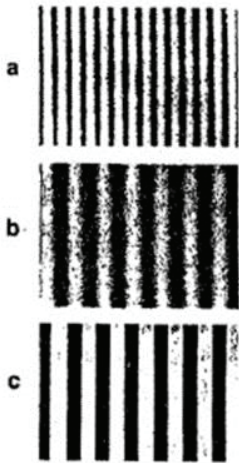


Figure 4.1 The Arden plates

The Cambridge gratings (Figure 4.2) use square-wave gratings at 4 cpd (a frequency at which human visual ability to discern contrast differences is the highest) and test 11 levels of contrast. Patients are shown 2 pages for each level of contrast and asked to identify which contains gratings and which is blank. The test is repeated 4 times and the score averaged. This test is administered at 6 meters, which is not always practical in a clinic setting or a doctor's office. There is a high probability of correct guessing with only 2 answer choices. (Richman, 2013)

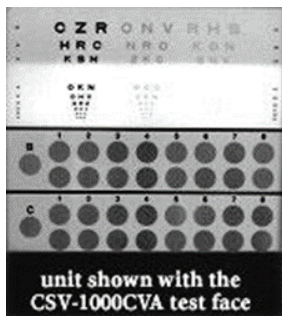


Figure 4.2 The Cambridge gratings

Ginsburg created several charts requiring patients to identify the orientation of sine-wave gratings as vertical, diagonally left, or diagonally right. These charts assess 5 spatial frequencies and 9 levels of contrast for each frequency. The last contrast level correctly identified determines the contrast sensitivity score for each frequency. The original *Vistech* (Figure 4.3) is not a true forced-choice test as a blank answer is available. The decrease in contrast levels is not uniform, but the average step size is about 0.23 log unit or a 70% decrease between levels. (Richman, 2013)

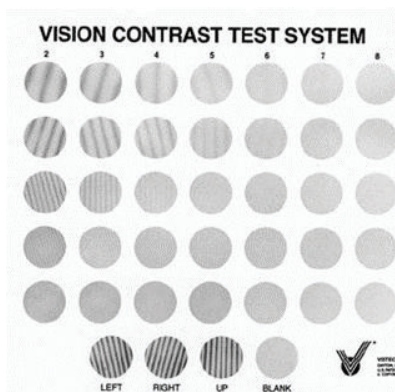


Figure 4.3 Vistech

The Functional Acuity Contrast Test (FACT (Figure 4.4)) is a modification of Vistech. It uses a smaller decrease between each contrast level (0.15 log unit or a 41% decrease) than Vistech and each circular patch of contrast gratings has smooth edges. However, the FACT does not increase the number of patches, and with a smaller step size between each level, a ceiling effect is created. (Richman, 2013)

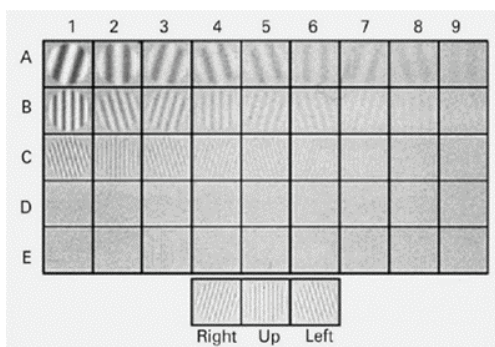


Figure 4.4 The Functional Acuity Contrast Test

These charts have poor test-retest reliability. They have a high probability of correct guessing with only 3 answer choices. Vector Vision's CSV-1000 (Figure 4.5) is a distance grating chart with internal retroillumination. The retroillumination may decrease the uneven lighting that often occurs with the other contrast charts. Four spatial frequencies are tested, using 9 contrast levels for each frequency. The contrast levels range from 0.5% contrast to 67% contrast and decrease by about 0.16 log unit between each level. At each contrast level, patients are shown 2 patches and are asked to identify the 1 with the contrast gratings. The lighting system is an advantage. However, having only 2 choices at each level creates a 50% chance of guessing correctly. (Richman, 2013)



Figure 4.5 Vector Vision's CSV-1000

4.2.2 Letter Charts

The Regan charts (Figure 4.6) evaluate visual acuity at contrast levels of 96%, 25%, and 11%. Each row of letters becomes smaller, allowing different spatial frequencies to be tested. The Regan charts do not have equal spacing between letters. For the larger rows of letters (smaller spatial frequency), the contrast levels tested are often too easily seen and do not approach patients' contrast threshold. At the higher spatial frequencies, these contrast levels can be used to determine contrast threshold; however, this information overlaps with that provided by standard Snellen-type acuity charts. (Richman, 2013)

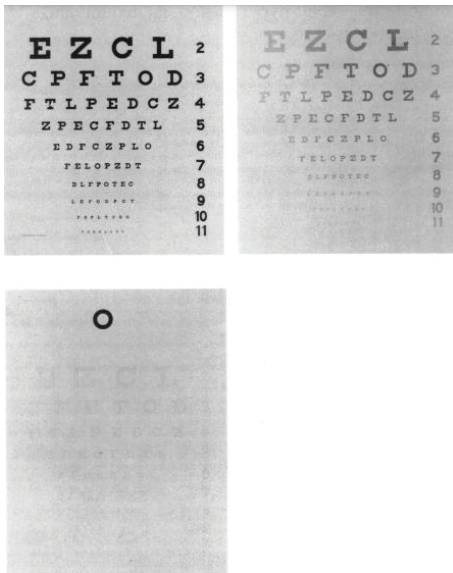


Figure 4.6 The Regan charts

The Pelli-Robson contrast sensitivity (Figure 4.7) chart uses Sloan letters 16 arranged in 16 groups of 3 letters. All letters are 20/630 and occupy 1.0 cpd at the manufacturer's specified testing distance of 1 meter. The contrast decreases by 0.15 log unit each triplet. Patients have to identify 2 of the 3 letters correctly to get credit for each triplet. The Pelli-Robson chart has a wide range of contrast, from 100% to 0.56%. It is quick, reliable, and easy to understand. Although some learning effect is possible with repeated testing, the option of 10 Sloan letters makes correct guessing unlikely. However, as with all charts, technical problems include unevenness of illumination, fading of the print, reflections from the surface, and the need to recognize letters. (Richman, 2013)



Figure 4.7 The Pelli-Robson contrast sensitivity chart

The Mars test (Figure 4.8) is similar in design to the Pelli-Robson chart as they both use Sloan letters. The contrast decreases by 0.04 log unit for adjacent letters, not triplets. The range of contrast tested is 91% to 1.2%. The Mars chart is smaller than the Pelli-Robson and used for near testing, specifically 0.5 meter. The test ends when patients identify 2 consecutive letters incorrectly. (Richman, 2013)



Figure 4.8 The Mars test

4.2.3 Computer-Based Testing

Computer-based contrast tests present advantages and disadvantages. Advantages include flexibility of programming to display contrast targets in a random pattern, alter the contrast between levels, and use a staircase strategy to bracket the contrast threshold. Disadvantages relate to the cost of the computer or cathode ray tube, the size and variable brightness of the monitor screen, and the time to complete the test. Also, a computer monitor's luminance must be calibrated prior to testing to ensure accurate contrast levels. Cathode ray tubes were originally used to create gratings starting in the 1960s. Cambridge Research

Systems currently offers hard ware to evaluate contrast sensitivity using cathode ray tubes. Their system tracks eye movements, calibrates the display luminance, and allows the parameters for testing to be chosen. Cambridge Research Systems offers contrast sensitivity testing as part of their Precision vision testing. (Richman, 2013)

The Freiburg Visual Acuity and Contrast Test (FrACT (Figure 4.9)) is a computer program that can be used on a cathode ray tube or an anti-aliasing computer monitor. It presents the Landolt C in 4 or 8 positions and patients are asked to identify the opening of the letter. The spatial frequency is determined by the size of the Landolt C. Threshold is determined by a bracketing technique using a best parameter estimation by sequential testing (Best PEST). (Richman, 2013)

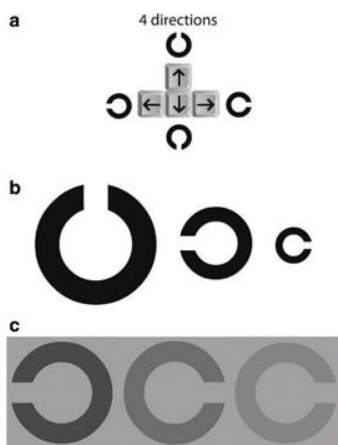


Figure 4.9 The Freiburg Visual Acuity and Contrast Test

The Holladay automated contrast sensitivity system (Figure 4.10) uses concentric circles of varying frequencies (similar to a bull's eye). The program starts at 50% contrast and decreases by increments of

0.3 log unit with each correct answer. The program shows the bull's eye of varying contrast or a blank screen. When an incorrect answer is given, smaller steps are used to bracket the contrast threshold. A bull's-eye target has been shown to have lower contrast sensitivity values than vertical sine-wave gratings. (Richman, 2013)



Figure 4.10 The Holladay automated contrast sensitivity system

There are also numerous contrast sensitivity charts that have been converted to testing on a computer monitor. *The Medmont AT-20* tests visual acuity at 8 contrast levels. *The Mentor B-VAT II* uses acuity charts at 9 contrast levels. The *LSV Acuity Program* presents a single letter whose contrast can be reduced to 30%. The Visual Capacity Analyzer presents letters of varying size and contrast. The *CST 1800 Digital contrast sensitivity tester* and *Optec 6500* contain the FACT chart and an acuity chart. (Richman, 2013)

SPARCS

SPARCS (Figure 4.11) is a novel, internet-based test designed to determine the contrast threshold of patients' central vision and peripheral vision. It is performed on a standard computer with internet access. It is designed to be used on a monitor set to 1024×768 resolution, 256 grey levels and a size of at least 22 cm width and 26.5 cm height. SPARCS can be accessed via <https://www.sparcscontrastcenter.com> where each patient gets a unique identification number. The website provides instructions on how to take the test. Patients are seated 50 cm from the computer monitor. At this testing distance, the test occupies 30° of vision horizontally and 23.5° of vision vertically. The central test area subtends 5° horizontally and 3.5° vertically. Patients are instructed to fixate on the central area and identify which of the areas appears different. When patients are ready, they click on the central area. Vertical square wave gratings with a spatial frequency of 0.4 cycles per degree appear for 0.3 s in one of the five tested areas. Patients then temporarily break fixation to select the area. Subsequently, patients fixate again on the central area and click it to activate the program to show the next image. The area with the gratings appears at random. Correct and incorrect responses are recorded by SPARCS until the contrast threshold is determined in each area. The contrast threshold is determined using a staircase strategy with reversals. Initial correct

responses advance four levels until an incorrect response is made. After the incorrect response, the contrast level presented is two levels easier. Thereafter, the algorithm advances or regresses one level at a time until two incorrect responses are made at a specific level, which establishes the threshold. If a patient stops trying to guess the correct area and simply clicks the same location again and again, the test terminates and explains to the patient to attempt to choose the location the image appeared. The range of contrast tested is from 100% to 0.45% (log contrast sensitivity 0.00 to 2.35) and decreases by approximately 0.15 log units between levels. The contrast value is calculated by Weber contrast. The central area and four peripheral areas each receive separate scores. Each log-based score is then scaled out of 20 by dividing by 2.35 and multiplying by 20. A total SPARCS score is summated from each of the five areas, making 100 the perfect summed score from all five areas. (Richman, 2013; 2014)

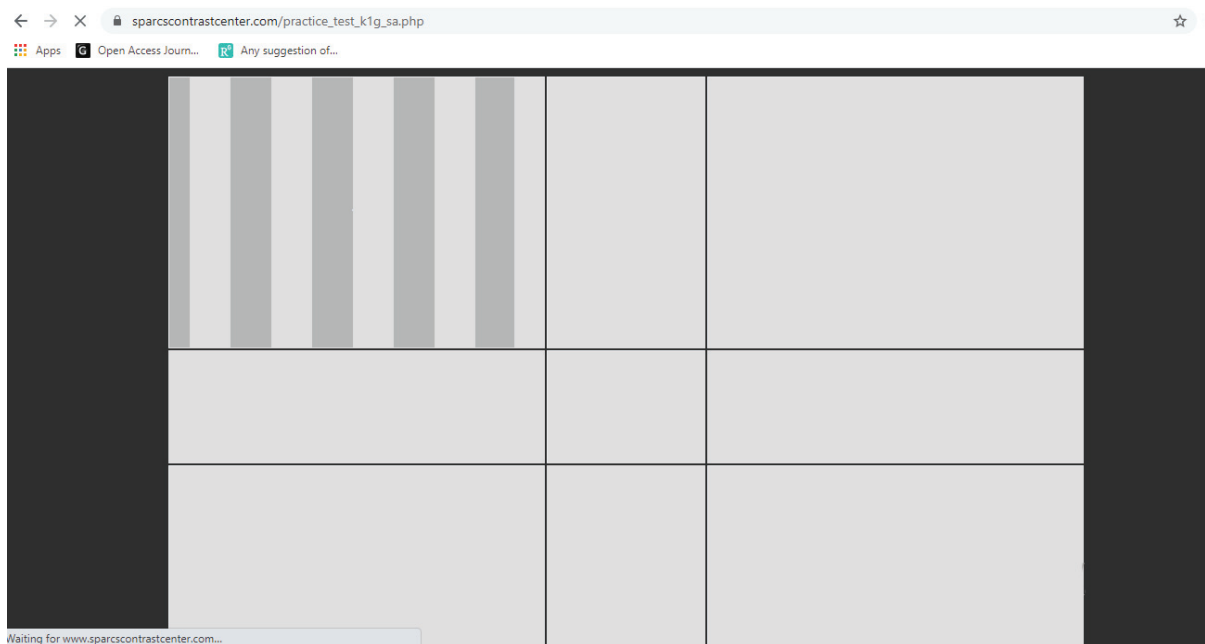


Figure 4.11 SPARCS

5. LINEAR REGRESSION ANALYSIS

5.1 Background

Statistics is a useful tool in medicine for description and inference of collected data. Inferential statistics are used to answer questions about the data, to generate a measure of effect, typically a ratio of rates or risks, to describe associations (correlations) to test hypotheses (formulating the alternative or null hypotheses), or to model relationships (regression) within the data and, in many other functions. Parameter estimates are the measures of associations and of the magnitude

of effects. The sources of potential bias are confounding, selection bias, measurement errors and random errors. The random error is estimated by p -. Confidence interval is the range of values, for which the p -value exceeds a specified alpha level (typically 0.05). The Bayesian approach uses data to improve hypothesized (prior) estimates in light of new data. All approaches require careful interpretation of assumptions and results. (Alexopoulos, 2010; Rothman, 1998; Altman, 1991))

The purpose of data analysis is to estimate with accuracy a parameter for the association under investigation, between a dependent variable (Y) and explanatory variables (Xi). A way to do this is to apply regression analysis in order to *model* the relationship. There are many types of regression analysis, which depend on the distribution of Y; if it is continuous and approximately normal we use linear regression model; if Poisson or multinomial we use log-linear analysis; if dichotomous we use logistic regression; if time-to-event data in the presence of censored cases (survival-type) we use Cox regression as a method for modeling. With this way, we try to predict the outcome (Y) based on values of a set of predictor variables (Xi). With these methods we can assess the impact of many variables (covariates and factors) in the same model. (Alexopoulos, 2010; Rosner, 1995; Draper, 1998)

5.2 Simple Linear equation

The model that best describes the dependent variable could be found by plotting the data. If the plot resembles a mathematical function you recognize, fit the data to that type of model. The continuous variables that appear to have linear relationship can be analyzed with a simple linear regression model but in the case that the variables are not linearly related, data transformation might be applied to satisfy the assumptions. If after the transformation, data don't follow the normal distribution, a GLM model may be needed. Alternatively, if it is not obvious which model best fits the data, an option is to try several models and select among them. (Alexopoulos, 2010; Draper, 1998; Munro, 2005)

The most appropriate model could be a straight line, a logarithmic, a higher degree polynomial or exponential. In order to find an appropriate model we could use the forward method in which we start by assuming the very simple model i.e. a straight line ($Y = a + bX$ or $Y = b_0 + b_1X$) and we find the best estimate. If this model does not fit the data sufficiently, then a more complicated model must be assumed e.g. a 2nd degree polynomial ($Y = a + bX + cX^2$). Another way is in a backward technique, where a complicated model is assumed e.g. a high degree polynomial, and we try to simplify it. We might also use a model suggested by theory or experience. Often a straight line relationship fits the data satisfactory and this is the case of simple linear regression. The simplest case of linear regression analysis is the model with one predictor variable. (Alexopoulos, 2010; Stijnen, 1999)

5.3 Linear regression equation

The purpose of regression is to predict a continuous variable Y on the basis of X or to describe how Y depends on X (regression line or curve such as Quadratic or Cubic)

$$X_1, X_2, \dots, X_k \Rightarrow Y$$

The Y is defined as "dependent", "response" or "outcome" variable, while X_i $i=1, \dots, k$ is defined as "predictor", "explanatory" or "independent" variable.

Assuming a linear relation in population, mean of Y for given X equals $\alpha + \beta X$ i.e. the "population regression line".

If $E(Y_i) = a + bX_i + e_i$ is the estimated line, then the fitted

$E(\hat{Y}_i) = a + bX_i$ is called the fitted (or predicted) value, and $E(Y_i) - E(\hat{Y}_i)$ is called the residual.

The estimated regression line is determined by the least squares estimation method that estimates parameters that minimize the sum of squared residuals (SSR). This is called the "least squares" method. In the equation

$$E(\hat{Y}_i) = a + bX_i$$

a is the intercept (often has no direct practical meaning)

b is the slope (the average increase of outcome per unit increase of predictor)

$$\hat{\alpha} = \bar{Y} - \hat{\beta}\bar{X}$$

$$\hat{\beta} = \frac{\sum_{i=1}^n (Y_i - \bar{Y})(X_i - \bar{X})}{\sum_{i=1}^n (X_i - \bar{X})^2}$$

$Y_i = a + bX_i + \sigma_{res}$ where σ_{res} = residual standard deviation = sd

Further assumptions about regression line includes the estimation of 95 % confidence interval (95%CI) for the slope b. The calculation is based on the standard error of b:

$$se(b) = \frac{S_{res}}{\sqrt{S_{xx}}} = \frac{S_{res}}{\sqrt{\sum x_i^2 - (\sum x)^2 / n}}$$

so, 95% CI for β is $b \pm t_{0.975} * se(b)$ [t-distr. with df = n-2]

and the test for $H_0: \beta=0$, is $t = b / se(b)$ [p-value derived from t-distr. with df = n-2]. Where n the number of observations

If the p value lies above 0.05 then the null hypothesis is not rejected which means that a straight line model in X does not help predicting Y. There is the possibility that the straight line model holds (slope = 0) or there is a curved relation with zero linear component. On the other hand, if the null hypothesis is rejected either the straight line model holds or in a curved relationship the straight line model helps, but is not the best model. The standard deviation of residual (σ_{res}) is estimated by

$$\sigma_{res} = \sqrt{\frac{\sum (residuals)^2}{n-2}} \text{ or } \sqrt{\frac{\sum (Y_i - Y_{fit})^2}{n-2}}$$

The standard deviation of residual (σ_{res}) characterizes the variability around the regression line i.e. the smaller the σ_{res} , the better the fit. It has a number of degrees of freedom. This is the number to divide by in order to have an unbiased estimate of the variance. In this case df = n-2, because two parameters, α and β , are estimated. (Alexopoulos, 2010)

5.4 Multiple linear regression analysis

In the multiple linear regression model, we have our dependent continuous Y variable, and more than one independent variables X_1, X_2, \dots, X_p as the predictor. Usually the questions of interest are how to predict Y on the basis of the X's and what is the "independent" influence of one variable corrected for other related variables? These questions can in principle be answered by multiple linear regression analysis. Y has normal distribution with mean

$$Y = \beta_0 + \beta_1 X_1 + \dots + \beta_p X_p + \sigma(Y), \text{ sd}(Y) = \sigma \text{ (independent of X's)}$$

The model parameters $\beta_0 + \beta_1 + \dots + \beta_p$ and σ must be estimated from data.

β_0 = intercept

$\beta_1 \dots \beta_p$ = regression coefficients

$\sigma = \sigma_{\text{res}}$ = residual standard deviation (Alexopoulos, 2010)

5.5 Assumptions

The assumptions of a linear model are: 1) Normality (for each value of the independent variable, the distribution of the dependent variable must be normal); 2) Homoscedasticity (the variance of the distribution of the dependent variable should be constant for all values of the independent variable); 3) Linearity (the relationship between the dependent variable and the independent variables should be linear, and all observations should be independent). So the assumptions are: independence; linearity; normality; homoscedasticity. In other words the residuals of a good model should be normally and randomly distributed i.e. the unknown does not depend on X ("homoscedasticity"). (Alexopoulos, 2010; Altman, 1991; Draper, 1998; Shedecor, 1989)

5.6 Checking for violations of model assumptions

To check model assumptions we used residual analysis. The most commonly used are the standardized residuals (ZRESID/ A standardized residual is a ratio: The difference between the observed count and the expected count and the standard deviation of the expected count in chi-square testing) and the studentized residuals (SRESID/ A studentized residual is calculated by dividing the residual by an estimate of its standard deviation). If we have a correct model, the residuals should have a normal distribution with mean zero and constant sd (i.e. not depending on X). We can check this by plotting the residuals against X. If the variation changes with increasing X, then there is violation of homoscedasticity. In addition, the Durbin-Watson test can be used for serial correlation of the residuals and casewise diagnostics for the cases meeting the selection criterion (outliers above n standard deviations). The residuals are normally distributed, (zero mean) independent, with constant standard deviation (homogeneity of variances).

To discover deviations from linearity and homogeneity of variables we can plot residuals against each predictor or against predicted values. To check the normality of residuals we can use an histogram (with normal curve) or a normal probability plot.

The goodness-of-fit of the model is assessed by studying the residuals, looking for outliers, observations with high "leverage" and influential points (An outlier is an anomalous response value, whereas a leverage point has atypical values of one or more of the predictors. Influential data points are observations that exert an unusually large effect on the results of regression analysis). (Alexopoulos, 2010; Stijnen, 1999)

5.7 Deviations from model assumptions

We can use some tips to correct some deviation from model assumptions. In case of curvilinearity in one or more plots we could add quadratic term(s). In case of non-homogeneity of residual standard deviant, transformations may be applied: **log Y** if the variance of the residuals is proportional to predicted Y; **square root of Y** if Y distribution is Poisson-like; **1/Y** if the square of the variance of the residuals is proportional to predicted Y; **Y²** if the square of the variance of the residuals decreases with Y. If linearity and homogeneity hold then non-normality does not matter if the sample size is big enough ($n \geq 50-100$). If linearity but not homogeneity hold then estimates of β 's are correct, but not the standard errors. They can be corrected by computing the "robust" se's (sandwich, Huber's estimate). (Alexopoulos, 2010; Draper, 1998; Shedecor, 1989)

5.8 Goodness of fit

The goodness of fit test is a statistical hypothesis test to see how well sample data fit a distribution from a population with a normal distribution. Goodness-of-fit establishes the discrepancy between the observed values and those that would be expected of the model in a normal distribution case.

5.9 Selection methods for Linear Regression modeling

There are several selection methods for linear regression modeling in order to find independent variables, so a variety of regression models from the same set of variables could be constructed. Forward variable selection enters the variables in the block one at a time based on entry prespecified criteria. Backward variable elimination enters all of the variables in the block in a single step and then removes them one at a time based on removal prespecified criteria. Stepwise variable entry and removal examines the variables in the block at each step for entry or removal. All variables must pass the tolerance prespecified criterion to be entered in the equation, regardless of the entry method specified. A variable is not entered if it would cause the tolerance of another variable already in the model to drop below the tolerance criterion. In a model fitting the variables entered and removed from the model and various goodness-of-fit statistics are displayed such as R², R squared change, standard error of the estimate, and an analysis-of-variance table.

6. LINEAR MIXED MODELS ANALYSIS

Linear mixed models are an extension of simple linear models, in non-independent data, to allow both fixed and random effects, and are particularly used when there is, that may arise from a hierarchical structure or in repeated measurement over a time period.

When there are multiple levels, the variability in the outcome can be either within groups or between groups. There are multiple ways to deal with such forms of data. One simple approach is to aggregate, so this aggregated data would then be independent.

Although aggregate data analysis yields consistent and effect estimates and standard errors, it does not really take advantage of all the data, because data are simply averaged.

Another approach to hierarchical data analysis is analyzing data from one unit at a time. Again although this does work, there are many models, and each one does not take advantage of the information in data. This can also make the results “noisy” in that the estimates from each model are not based on very much data.

Linear mixed models (LMM, also called multilevel models) can inbetween these two approaches. The individual regressions include many estimates and lots of data, but are noisy. The aggregate option is less noisy, but may lose important differences by averaging all samples within each part. (Snijders, 2012; Singer, 2003)

6.1 Random Effects

Mixed models incorporate both fixed and random effects. A fixed effect is a parameter that does not vary. For example, we may assume there is some true regression line in the population, β , and we get some estimate of it, $\hat{\beta}$. In contrast, random effects are parameters that are themselves random variables. For example, we could say that β is distributed as a random normal variate with mean μ and standard deviation σ , or in equation form:

$$\beta \sim N(\mu, \sigma)$$

This is such as linear regression, where the data are random variables, but the parameters are fixed effects, but now the data are random variables, and the parameters are random variables (at one level), but fixed at the highest level. (Snijders, 2012; Singer, 2003)

$$Y = X\beta + Zu + \epsilon$$

Where Y is a $N \times 1$ column vector, the outcome variable; X is a $N \times p$ matrix of the p predictor variables; β is a $p \times 1$ column vector of the fixed-effects regression coefficients (the β s); Z is the $N \times qJ$ design matrix for the q random effects and J groups; u is a $qJ \times 1$ vector of q random effects (the random complement to the fixed β) for J groups; and ϵ is a $N \times 1$ column vector of the residuals, that part of y that is not explained by the model, $X\beta + Zu$. (Snijders, 2012; Singer, 2003) To recap:

$$\underbrace{N \times 1}_{\mathbf{y}} = \underbrace{\underbrace{N \times 1}_{\mathbf{X}} \underbrace{p \times 1}_{\mathbf{\beta}}}_{N \times p} + \underbrace{\underbrace{N \times 1}_{\mathbf{Z}} \underbrace{qJ \times 1}_{\mathbf{u}}}_{N \times qJ} + \underbrace{N \times 1}_{\mathbf{\epsilon}}$$

7. SCOPE

The aim of this study is to measure contrast sensitivity with a new method (SPARCS) in subjects who underwent femto laser in situ keratomileusis (LASIK), in subjects with photorefractive keratectomy (PRK) and in “healthy” controls (persons who do not have a refractive error and have not undergone any refractive surgery). We wanted to study whether there are differences in SPARCS results among our groups.

8. INTRODUCTION

Ocular perception of environment depends on optical and neural factors (Campbell, 1965). The most common ocular disorders, affecting all age groups, are refractive errors (Hashemi, 2018). The estimated prevalence of uncorrected refractive errors worldwide is 153 million people (WHO, 2006). Refractive errors occur because of a disproportion in ocular anatomy, so the eye cannot clearly focus the images from the outside world on the retina (Richter, 2017). The result of refractive errors is blurred vision, which is sometimes so severe that it causes visual impairment (Mastrangelo, 2020). The most common refractive errors are: myopia, hyperopia and astigmatism (WHO, 2006).

Laser refractive eye surgery is used to reshape cornea's curvature in order to correct refractive errors and to decrease dependency on glasses or contact lenses, by restoring the refractive power of the eye. The two most widely used techniques of laser refractive eye surgery are photorefractive keratectomy (PRK) and laser in situ keratomileusis (LASIK) (Muruet, 2018).

A number of studies measuring patient satisfaction rates after LASIK and PRK surgery have been published. Apart from uncorrected visual acuity results, contrast sensitivity and higher-order aberrations (Manche, 2011) may decrease patients' satisfaction rates and quality of vision after a laser refractive eye surgery.

As described by Richman et al (Richman, 2013) contrast is a measure of the amount of lightness or darkness an object has in comparison to its background. Contrast threshold is the smallest difference in lightness and darkness between an object and its background that can be distinguished. Contrast threshold is typically reported as contrast sensitivity, which is the inverse of the contrast threshold (Richman, 2013). It is a more sensitive visual test that has the ability to detect visual abnormalities in subjects with normal visual acuity but complaining of visual disturbances (Barboni, 2013). It is a useful way of estimating people's functional vision since it influences many of its aspects, such as VA, visual field, motion detection, dark adaptation, and pattern recognition. Decreased CS may disturb people's everyday life (Gupta, 2017).

The Spaeth/Richman Contrast Sensitivity ('SPARCS') test is an internet-based contrast measurement tool. Black stripes decrease in contrast becoming fainter and harder to see until they blend with the white background. Measurements are assessed in five areas of the visual field. It evaluates CS centrally and in four peripheral quadrants and scores them separately. Because it contains contrast gratings instead of

letters, low literacy level subjects may be tested as reliably as literate ones. The five areas are presented in two irregular sequences, so even with retesting, memorizing the answer sequence is unlikely. The test takes an average of 3 minutes per eye. The eye not being tested is covered with a patch (Gupta, 2013).

9. MATERIALS AND METHODS

9.1 Study design and Population

This is a retrospective study, which was approved by the Scientific Council of 401 General Military Hospital of Athens and was conducted in accordance with the Declaration of Helsinki at the Ophthalmologic Clinic of 401 General Military Hospital of Athens. Recruiting and testing took place between November 2019 and December 2020.

We studied three groups: "healthy" controls and individuals who underwent a myopic refractive surgery either Femto LASIK or PRK, using the SPARCS contrast sensitivity test. Sixty-two eyes of 31 individuals were included in each group. All the subjects were thoroughly informed about the nature of the investigation and provided their consent before the start of their examination. Inclusion criteria included people aged above 21 years, uncorrected visual acuity of 20/20 free individual history, time since the refractive surgery had to be more than 1 year, less than 0.50 D spherical equivalent and tomography without terrain points. Exclusion criteria included Intraocular Pressure more than 20 mmHg, any ocular pathology, history of neurological diseases, any tropia or phoria, history of previous ophthalmic surgery (excluding refractive surgery), re-intervention history for correction of residual refractive error, ocular surface disease, and color vision deficiency. 200 patients were approached of which 120 were examined and 100 were eligible to participate in our study. Of these, 93 managed to complete the test. Data were analyzed for 186 eyes from 93 subjects.

9.2 Outcome Measurements and data collection

Demographic information (age, gender, educational level, smoking habits) and an ocular medical history were obtained and documented for all study participants through a questionnaire-structured interview conducted by the main investigator. All subjects were given a comprehensive ophthalmic clinical examination from the main investigator which included (1) Snellen VA (2) refraction, (3) color vision via Ishihara charts, (4) intraocular pressure via Goldmann Applanation tonometry, (5) a slit-lamp and fundus examination and (6) SPARCS test. *Table 9.1* shows the way that data were collected.

id	continuous	measurement
eye	categorical	scale 0=right 1=left

age	continuous	in years		
gender	categorical	0=male	1=female	
surgery	categorical	0=controls	1=PRK	2=LASIK
smoking	categorical	0=no	1=yes	

Table 9.1 Data collection

9.2.1 CS Assessment

The test was applied using a Lenovo, ideapad, 19'', touchscreen. The same technician explained and administered the test to all participants. Each subject was administered the SPARCS test monocularly twice. Individuals had a first exercise test and then the second's test's results was recorded. Every individual was tested on the "Practice Test" of SPARCS Contrast Sensitivity test. The non-tested eye was covered with an occluder. All tests were conducted in the same room for every individual, which was of low lighting to minimize glare and reflections and ensure uniform testing conditions. The subject was instructed to maintain fixation on the central area throughout the test. Central fixation was verified by the trained technician who observed the subject during the testing period. If fixation was not acceptable, the test was restarted.

9.2.2 SPARCS

As described by Richman et al (Richman, 2013; 2015) SPARCS is a new internet-based assessment of CS, which can be accessed at <https://www.sparscontrastcenter.com>. Detailed test instructions and a unique ID are provided on the website. The test can be performed using a standard web-browser on a computer with a monitor set to 1024 × 768 resolution, 256 gray levels, and a monitor size at least 22 cm wide and 26.5 cm high. The computer screen is divided into 9 rectangle areas with two parallel horizontal lines and 2 parallel vertical lines. The online test has a screen standardization setting to rescale the screen such that the center rectangle is 4.4 cm wide. At the prescribed viewing distance of 50 cm, the test occupies 30° of vision horizontally and 23.5° of vision vertically, and, in the central test area, 5° of vision horizontally and 3.5° of vision vertically. SPARCS evaluates CS in five areas of the visual field: the left upper quadrant (LUQ), left lower quadrant (LLQ), right upper quadrant (RUQ), right lower quadrant (RLQ), and central area. During the test, an image is displayed in one of the 5 testing areas at random for 0.3 s, while the other 4 areas stay a similar color to the background. This image consists of square wave gratings in the form of vertical dark bars on a constant light background at a fixed spatial frequency of 0.4 cycles per degree. During the test, the luminance of the gratings is gradually decreased. Seventeen

potential levels of contrast can be tested. Contrast decreases by ~ 0.15 log units between levels and ranges from 100 to 0.45% (log CS 0.00 to 2.35). The subject selects which area the vertical dark bars appeared (LUQ, LLQ, RUQ, RLQ, or center). The testing strategy uses a staircase method with reversals as described by Richman et al. In the beginning, correct responses allow the subject to advance 4 levels until an incorrect response is made. Then, the algorithm presents a contrast level that is 2 levels easier. The test then advances or regresses 1 level at a time until the subject makes 2 incorrect responses at a certain contrast level. This establishes the contrast threshold for the testing area. In areas where the threshold has been reached, contrast levels plus or minus one level of the threshold are presented at random until a threshold has been determined for all the remaining test areas, at which point the test is complete. Each of the 5 testing region's log-based scores are scaled 0 to 20, making the highest possible SPARCS score to be 100.

9.3 STATISTICAL ANALYSIS

Data was analyzed using the Stata statistical software package version 13 (STATA Corp., College Station, TX). Normal distribution of demographic and clinical information was assessed by plots (histogram and probability graphs) and corresponding statistical tests (Kolmogorov–Smirnov/Shapiro–Wilk test). (Appendix 2 Normally distributed continuous data are summarized as mean ± standard deviation (SD), and non-normally distributed as median with 25° and 75° percentile, as appropriate. Discrete data are presented as Number (N) and percentage. We created a new variable named peripheral which is the sum of LUQ, LLQ, RUQ and RLQ. The association between the scores (total, center, peripheral) and refractive surgery were investigated using univariate and multivariate linear regression analysis and for each eye separately and then for both eyes together. R² and adjusted R² were estimated for each model.

$$R^2 = \frac{SS_{\text{reg}}}{SS_{\text{tot}}} \quad \text{and} \quad \bar{R}^2 = 1 - \frac{SS_{\text{res}}/df_e}{SS_{\text{tot}}/df_t}$$

Subsequently, results were compared with those from mixed effects linear regression to account for correlation among eyes from the same subject in the analysis including both eyes per participant. Likelihood Ratio test was used to estimate the best model. For all statistical tests, the P value <0.05 was considered statistically significant. We assessed model assumption for all models. (Appendix 3)

10. RESULTS

Data's distributions were checked with Kolmogorov smirnov and Swilk tests (*Table 10.1*) and histograms (*Figure 10.1*). We considered center, peripheral and total variables that follows normal distribution.

	swilk	ksmirnov
<i>age</i>	<0.001	<0.001
<i>center</i>	0.28385	0.009
<i>peripheral</i>	0.00022	0.174
<i>total</i>	0.07369	0.349
<i>LLQ</i>	0.01175	0.011
<i>LUQ</i>	0.04171	<0.001
<i>RLQ</i>	0.01538	0.009
<i>RUQ</i>	<0.001	<0.001
<i>D</i>	<0.001	<0.001

Table 10.1 Results after testing data's distributions

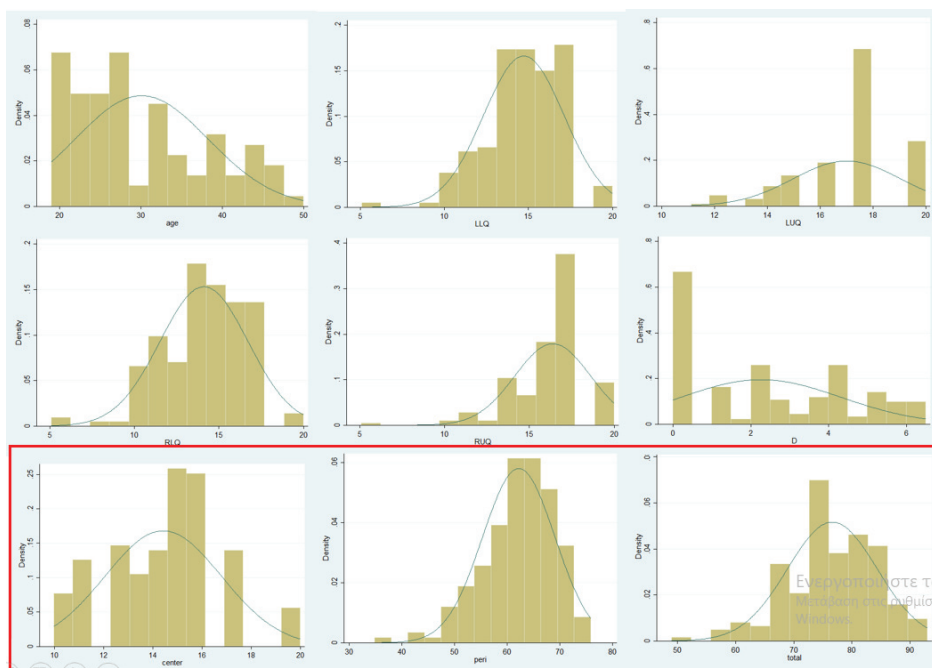


Figure 10.1 Data's distribution as presented on histograms

The control group included 62 eyes from 31 subjects (25 males and 6 females), Femto-LASIK group 62 eyes from 31 subjects (15 males and 16 females) and the PRK group included 62 eyes from 31 subjects (19 males and 12 females). *Table 10.2* presents the participants' demographics and SPARCS scores, overall and by surgical category.

		Total (N=93)	Control (N=31)	PRK (N=31)	LASIK (N=31)	
Demographic Data	Age, years (median, 25 ^o -75 ^o)	27 (23-36)	27 (25-36)	27 (22-39)	27 (22-37)	
	Gender (N, %)	<i>Male</i>	118(63.44)	25 (42.37)	19 (32.2)	15(25.42)
		<i>Female</i>	68(36.56)	6 (17.65)	12 (35.29)	16(47.06)
	Smoking (N, %)	<i>Yes</i>	48(25.81)	21 (30.43)	24 (34.78)	24 (34.78)
		<i>No</i>	138(74.19)	10 (41.67)	7 (29.17)	7 (29.17)
Diopters (median, 25 ^o -75 ^o)		2 (0-4)	0	3.5(2-5)	3.75(2-4)	
SPARCS scores	center (mean ± SD)	14.4±2.4	15.4±2.4	13.4±2.2	14.4±2	
	LUQ (median, 25 ^o -75 ^o)	17.43 (15.93, 17.43)	17.43 (15.93, 17.43)	17.43 (14.04, 17.43)	17.43 (15.93, 17.43)	
	LLQ (median, 25 ^o -75 ^o)	14.87 (13.37, 15.93)	14.87 (14.04, 17.43)	14.04 (12.3, 15.93)	14.87 (13.37, 15.93)	
	RUQ (median, 25 ^o -75 ^o)	17.43 (14.87, 17.43)	17.43 (15.93, 17.43)	15.93 (14.87, 17.43)	17.43 (14.87, 17.43)	
	RLQ (median, 25 ^o -75 ^o)	14.57 (12.3, 15.93)	14.87 (14.04, 15.93)	13.37 (11.12, 14.87)	14.57 (12.3, 15.93)	
	peripheral (mean ± SD)	62.9±6.8	64.4±5.8	59.5±7	62.8±6.9	
	total (mean ± SD)	76.6±7.7	79.8±6	73±7.6	77±8	

Table 10.2 Participants' demographics and SPARCS scores, overall and by surgical category.

We compared univariate vs multivariable linear regression analysis for the different scores of SPARCS (Total, Central and Peripheral) counting only left or right eye or both eyes. The results are presented in Table 10.3. PRK had always statistical significant difference compared with control group and this relationship didn't change even after adjusting for all our confounders, for which we didn't find any statistically significant relationship. On the other hand, Lasik had bordered statistically significant difference on when we used both eyes for our analysis without accounting for the dependence that both eyes correspond to the same individual.

		Both eyes	Right eye	Left eye
Total	Multivariate	$R^2=0.1651/adjR^2=0.1371$	$R^2=0.207/adjR^2=0.1517$	$R^2=0.1413/adjR^2=0.0814$

	<i>PRK vs cntrl</i>	-9.2 (-13, -5.3) <0.001	-9.6 (-14.9, -4.2) 0.001	-8.6 (-14.4, -2.9) 0.003
	<i>Lasik vs cntrl</i>	-4.7 (-8.6, -0.8), 0.017	-4.4 (-9.8, 1.1) 0.113	-4.9 (-10.8, 0.9) 0.094
	Univariate	$R^2=0.133/adjR^2=0.1235$	$R^2=0.1605/adjR^2=0.1418$	$R^2=0.1106/adjR^2=0.0909$
	<i>PRK vs cntrl</i>	-6.8 (-9.4, -4.3) <0.001	-7.3 (-10.9, -3.7) <0.001	-6.3 (-10.1, -2.6) 0.001
	<i>Lasik vs cntrl</i>	-2.6 (-5.2, -0.3) 0.047	-2.6 (-5.9, 1.2) 0.195	-2.8 (-6.6, 0.9) 0.137
Center	Multivariate	$R^2=0.1324/adjR^2=0.1033$	$R^2=0.1628/adjR^2=0.1044$	$R^2=0.1315/adjR^2=0.0536$
	<i>PRK vs cntrl</i>	-2.3 (-3.5, -1.1) <0.001	-2.6 (-4.4, -0.9) 0.004	-1.9 9-3.6, -0.2) 0.027
	<i>Lasik vs cntrl</i>	-1.2 (-2.5, -0.03) 0.044	-1.4 (-3.2, 0.4) 0.126	-1.1 (-2.8, 0.6) 0.191
	Univariate	$R^2=0.1141/adjR^2=0.1044$	$R^2=0.1231/adjR^2=0.1036$	$R^2=0.1066/adjR^2=0.0867$
	<i>PRK vs cntrl</i>	-2 (-2.8, -1.2) <0.001	-2.1 (-3.3, -0.9) 0.001	-1.8 (-2.9, -0.7) 0.002
	<i>Lasik vs cntrl</i>	-1 (-1.8, -0.2) 0.017	-1 (-2.1, 0.2) 0.111	-1 (-2.1, 0.1) 0.78
Periphery	Multivariate	$R^2=0.1397/adjR^2=0.1109$	$R^2=0.1907/adjR^2=0.1342$	$R^2=0.1289/adjR^2=0.0681$
	<i>PRK vs cntrl</i>	-7.2 (-10.7, -3.8) <0.001	-7.3 (-11.9, -2.7) 0.002	-6.9 (-12.3, -1.6) 0.011
	<i>Lasik vs cntrl</i>	-3.7 (-7.2, -0.1) 0.042	-3.3 (-8, 1.4) 0.168	-3.8 (-9.2, 1.6) 0.162
	Univariate	$R^2=0.0898/adjR^2=0.0799$	$R^2=0.119/adjR^2=0.0994$	$R^2=0.0687/adjR^2=0.0480$
	<i>PRK vs cntrl</i>	-4.9 (-7.3, -2.6) <0.001	-5.3 (-8.4, -2.2) 0.001	-4.6 (-8.2, -1) 0.012
	<i>Lasik vs cntrl</i>	-1.6 (-3.9, 0.7) 0.185	-1.3 (-4.5, 1.8) 0.394	-1.8 (-5.4, 1.8) 0.316

Table 10.3 Univariate and multivariable linear regression analysis results per score and for both eyes and by eye separately. Multivariate models are adjusted for age, changed diopters, smoking habits and gender.

We compared multivariate linear regression analysis vs mixed effect linear regression analysis among the different scores of SPARCS (Total, Central and Peripheral) when analyzing results for both eyes (Table 10.4).

In this analysis the mixed effects linear regression model was the optimal fir better accounting for the structure of the observation, (LR p-value<0.001). As a result we conclude that there was statistically significant difference between the PRK group and control group but there was not statistical significant difference between the Femto-LASIK group and the control group at every SPARCS score (Total, Central, Peripheral).

Total Mixed | |

	<i>PRK vs cntrl</i>	-5.9 (-9, -2.8) <0.001
	<i>Lasik vs cntrl</i>	-2.1 (-5.4, 1.1) 0.192
	Linear Both eye	
	<i>PRK vs cntrl</i>	-9.2 (-13, -5.3) <0.001
	<i>Lasik vs cntrl</i>	-4.7 (-8.6, -0.8), 0.017
Center	Mixed	
	<i>PRK vs cntrl</i>	-1.6 (-3, -0.3) 0.018
	<i>Lasik vs cntrl</i>	-0.7 (-2.1, 0.7) 0.326
	Linear Both eye	
	<i>PRK vs cntrl</i>	-2.3 (-3.5, -1.1) <0.001
	<i>Lasik vs cntrl</i>	-1.2 (-2.5, -0.03) 0.044
Periphery	Mixed	
	<i>PRK vs cntrl</i>	-5.5 (-9.4, -1.6) 0.006
	<i>Lasik vs cntrl</i>	-2.3 (-6.3, 1.8) 0.270
	Linear Both eye	
	<i>PRK vs cntrl</i>	-7.2 (-10.7, -3.8) <0.001
	<i>Lasik vs cntrl</i>	-3.7 (-7.2, -0.1) 0.042

*LR test vs. linear regression P-value < 0.001**

Table 10.4 Comparison between multivariable linear regression analysis vs mixed effect linear regression analysis. All models are adjusted for age, changed diopters, smoking habits and gender.

There was statistically significant difference between the PRK group and control group but not statistical significant difference between the Femto-LASIK group and the control group at every SPARCS score (Total, Central, and Peripheral). None of the covariates was SS. More specifically, the PRK group had a lower total score of 5.9 points (p-value <0.001), a lower central score of 1.6 points (p-value =0.018) and a lower peripheral score of 5.5 points (p-value =0.006) than control group.

11.DISCUSSION

As a first goal, our study aimed to compare contrast sensitivity with a novel internet-based test, SPARCS, which assesses low spatial frequency CS, in three samples, the first with fempto-LASIK refractive surgery, the second with PRK refractive surgery and the third with emmetropic eyes. We found that SPARCS mean total, central and peripheral scores were reduced both with PRK and LASIK. The finding that PRK cause a significant reduction in CS for peripheral vision, where LASIK doesn't is a new observation that may be of clinical importance. This shows the importance of testing both central and peripheral vision which can be assessed with the SPARCS test.

Contrast sensitivity is a significant side of visual function (Farahvash, 2008). Someone with 20/20 acuity may complain of poor vision, because of low contrast sensitivity. Contrast sensitivity test can be used to identify many ocular disorders. It plays a role in many aspects of vision, visual field, dark adaptation, specifically motion detection, pattern recognition, and visual acuity (Richman, 2013). Contrast sensitivity tests could study the quality of vision through information that is not provided by standard clinical visual acuity tests (Arden, 1978).

Many studies have investigated central contrast sensitivity after refractive surgery. Ghaith et al reported a significant reduction in contrast sensitivity after PRK (Ghaith, 1998). Carr et al reported an overall decrease in contrast sensitivity after LASIK in all spatial frequencies (Carr, 1998). Manche et al demonstrated that at 1 month postoperatively, LASIK had an advantage over PRK, but at postoperative month 3, the differences between PRK and LASIK results had resolved (Manche, 2011) Bryndon et al demonstrated that under well-controlled surgical conditions, PRK and thin-flap LASIK refractive surgeries achieve similar results (Hatch, 2011). Daizong et al conducted a metanalysis, which manifested that there were no statistically significant differences in visual outcomes (efficacy and safety) and visual quality (HOAs and CS). In addition FS-LASIK behaved better in predictability than other types of surgeries (Wen, 2017).

The effects of refractive surgeries on central CS have been analysed widely previously. To date, there was no definitive method to evaluate peripheral CS thresholds after refractive surgery. SPARCS is a new CS test that is able to test peripheral CS. It is a novel internet-based test, which assesses low spatial frequency CS. SPARCS is easy to perform, and has similar test–retest repeatability (Gupta, 2017). SPARCS eliminates potential confounders such as literacy, intelligence, and pattern recognition. It only requires a computer with Internet access and a web browser. SPARCS also has multiple answer choices reducing the probability of guessing correctly (Richman, 2013)

Derefeldt et al demonstrated that there was no significant difference between young and middle-aged subjects with regard to contrast sensitivity, but subjects aged 60 years or more showed significantly lower

contrast sensitivity (Derefeldt, 1979). Ross et al showed that in the age's range 50-87 years there was a linear decline in contrast sensitivity with age for medium and high spatial frequencies, but sensitivity for low spatial frequencies was independent of age (Ross, 1985). The age range of our patients was 19-50 years old. The same age and the age's range which was <50 years old, among our groups, got this confounder out of this study.

Brabyn and McGuinness (1979) found that females had higher sensitivity in the lower spatial frequencies and males had higher sensitivity in the higher spatial frequencies. A study by Abramov et al. (2012a) found that males had higher contrast sensitivity at all spatial frequencies, with greater differences at higher spatial frequencies (Vanston, 2017). We found that men had higher contrast sensitivity at all areas than women, but it was not statistically significant.

In a review, Heishma et al examined the effects of nicotine administration and cigarette smoking on human performance. They found no effect of smoking on visual contrast sensitivity (Heishma, 1994). In our study this confounder had also no statistically significant importance.

The present study isolated subjects with specific eye surgeries and excluded people with concurrent ocular diseases. In daily clinical practice, subjects often have more than one issue. Our results may have limited external validity as they have been performed on a highly selected patient sample according to the study criteria. The strict criteria were selected as previous information was scarce and we wanted to target a well defined population to be able to correctly account for the outcome and the underlying effects.

Future studies may need to test our approach to a wider samples

A limitation of our study pertains to its retrospective design. A prospective study better accounts for causality. In addition, we need to acknowledge the possible bias from the absence of pupil size and not ultimately controlled environment. Moreover, the diopters that were changed at each method ranged from 1 to 6.5 D, so we couldn't check if there is an effect between greater D change and CS. The small sample size of our groups is also a limitation resulting in limited statistical power. Larger and prospective studies are needed to better compare the central, peripheral and total contrast sensitivity after different refractive surgeries.

12. CONCLUSION

Following refractive surgery some patients complain of reduced ability to function visually, despite a level of visual acuity that would be expected to be satisfactory. The explanations for this have included the presence of high-order aberrations or worsening ability to discern contrast. We have performed a retrospective study to compare the effect of two different methods of performing refractive corneal

surgery on contrast sensitivity, specifically. We assessed Photorefractive keratectomy (PRK) and Laser-assisted in situ Keratomileusis (LASIK)., utilizing SPARCS for contrast assessment, an online method of assessing contrast sensitivity both centrally and peripherally The results indicate that both procedures reduce peripheral as well as central contrast sensitivity, built only with PRK did the change achieved statistical significance. The finding that keratorefractive surgery can reduce discernment of contrast peripherally has -to the best of our knowledge- not been previously demonstrated.

13.REFERENCES

Adler's Physiology of the Eye: Clinical application. Edited by: Kaufman, P., Albert, Alm. Philadelphia Mosby Tenth Edition, 2003.

Alexopoulos EC. Introduction to multivariate regression analysis. Hippokratia. 2010;14(Suppl 1):23-28.

Alpins, N (2002). "A re-analysis of astigmatism correction". The British Journal of Ophthalmology. 86 (7): 832. doi:10.1136/bjo.86.7.832a. PMC 1771183. PMID 12084766.

Alpins, NA (1993). "A new method of analyzing vectors for changes in astigmatism". Journal of Cataract and Refractive Surgery. 19 (4): 524–33. doi:10.1016/s0886-3350(13)80617-7. PMID 8355160.

Altman DG. Practical Statistics for Medical Research. Chapman & Hall/CRC, 1991.

Amar Agarwal; Athiya Agarwal; Soosan Jacob (14 May 2009). Refractive Surgery. Jaypee Brothers Publishers. p. 546. ISBN 978-81-8448-412-0.

Arden GB. The importance of measuring contrast sensitivity in cases of visual disturbance. Br J Ophthalmol. 1978 Apr;62(4):198-209. doi: 10.1136/bjo.62.4.198. PMID: 348230; PMCID: PMC1043188.

"Astigmatism". MedicineNet. OnHealth.com. Archived from the original on 2 July 2013. Retrieved 8 September 2013.

Barboni MT, Feitosa-Santana C, Barreto Junior J, Lago M, Bechara SJ, Alves MR, Ventura DF. Longitudinal measurements of luminance and chromatic contrast sensitivity: comparison between wavefront-guided LASIK and contralateral PRK for myopia. *Arq Bras Oftalmol*. 2013 Oct;76(5):270-3. doi: 10.1590/s0004-27492013000500003. PMID: 24232938.

Bekerman, Inessa, Paul Gottlieb, and Michael Vaiman. "Variations in eyeball diameters of the healthy adults." *Journal of ophthalmology* 2014 (2014).

Bron AJ, Tripathi DM, Tripathi BJ: Wolff's anatomy of the eye and orbit. London, Chapman & Hall Medical, 1997.

Campbell FW, Green DG. Optical and retinal factors affecting visual acuity. *J Physiol*. 1965;181(3):576-93.

Carr JD, Stulting RD, Sano Y, Thompson KP, Wiley W, Waring GO 3rd. Prospective comparison of single-zone and multizone laser in situ keratomileusis for the correction of low myopia. *Ophthalmology*. 1998 Aug;105(8):1504-11. doi: 10.1016/S0161-6420(98)98037-X. PMID: 9709766.

Christie, B.; Schweigerling, J.; Prince, S.; Silvestrini, T. (2005). "Optical Performance of a Corneal Inlay for Presbyopia". *Investigative Ophthalmology & Visual Science*. 46 (5): 695. Archived from the original on 2015-01-09.

Cunha-Vaz, J., R. Bernardes, and C. Lobo, Blood-retinal barrier. *Eur J Ophthalmol*, 2011. 21 Suppl 6: p. S3-9.

Cunningham, edited by Paul Riordan-Eva, Emmett T. (2011-05-17). *Vaughan & Asbury's General Ophthalmology* (18th ed.). New York: McGraw-Hill Medical. ISBN 978-0-07-163420-5.

Draper NR, Smith H. *Applied Regression Analysis*. Wiley Series in Probability and Statistics, 1998.

Derefeldt G, Lennerstrand G, Lundh B. Age variations in normal human contrast sensitivity. *Acta Ophthalmol (Copenh)*. 1979 Aug;57(4):679-90. doi: 10.1111/j.1755-3768.1979.tb00517.x. PMID: 525292

Dua, H.S., et al., Human corneal anatomy redefined: a novel pre-Descemet's layer (Dua's layer). *Ophthalmology*, 2013. 120(9): p. 1778-85.

Ehlers, N., Some comparative studies on the mammalian corneal epithelium. *Acta Ophthalmol (Copenh)*, 1970. 48(4): p. 821-8.

E. Peli (Oct 1990). "Contrast in Complex Images" (PDF). *Journal of the Optical Society of America A*. 7 (10): 2032–2040. doi:10.1364/JOSAA.7.002032. Archived from the original (PDF) on 2016-05-21. Retrieved 2009-02-16.

Eydelman, MB; Drum, B; Holladay, J; Hilmantel, G; Kezirian, G; Durrie, D; Stulting, RD; Sanders, D; Wong, B (2006). "Standardized analyses of correction of astigmatism by laser systems that reshape the cornea". *Journal of Refractive Surgery*. 22 (1): 81–95. doi:10.3928/1081-597X-20060101-16. PMID 16447941.

Fannin, Troy E., and Theodore Grosvenor. *Clinical optics*. Butterworth-Heinemann, 2013.

Farahvash MS, Mahmoudi AH, Farahvash MM, Tabatabaee A, Riazi M, Mohammadzadeh S, Faghihi H, Nilli-Ahmadabadi M, Mirshahi A, Karkhaneh R, Aalami-Harandi Z, Javadian A, Abdolahi A, Lashey A. The impact of macular laser photocoagulation on contrast sensitivity function in patients with clinically significant macular edema. *Arch Iran Med*. 2008 Mar;11(2):143-7. PMID: 18298289.

Foster PJ, Jiang Y (February 2014). "Epidemiology of myopia". *Eye*. 28 (2): 202–8. doi:10.1038/eye.2013.280. PMC 3930282. PMID 24406412.

Ghaith AA, Daniel J, Stulting RD, Thompson KP, Lynn M. Contrast sensitivity and glare disability after radial keratotomy and photorefractive keratectomy. *Arch Ophthalmol*. 1998 Jan;116(1):12-8. doi: 10.1001/archopht.116.1.12. PMID: 9445203.]

Gilbert Smolin; Charles Stephen Foster; Dimitri T. Azar; Claes H. Dohlman (2005). *Smolin and Thoft's The Cornea: Scientific Foundations and Clinical Practice*. Lippincott Williams & Wilkins. pp. 173–. ISBN 978-0-7817-4206-1.

Goldstein, E. Bruce, and James Brockmole. *Sensation and perception*. Cengage Learning, 2016.

Gupta L, Cvintal V, Delvadia R, Sun Y, Erdem E, Zangalli C, Lu L, Wizov SS, Richman J, Spaeth E, Spaeth GL. SPARCS and Pelli-Robson contrast sensitivity testing in normal controls and patients with cataract. *Eye (Lond)*. 2017 May;31(5):753-761. doi: 10.1038/eye.2016.319. Epub 2017 Jan 20. PMID: 28106888; PMCID: PMC5437330.

Hadrill, Marilyn. "LASIK Risks and LASIK Complications". AllAboutVision.com. Retrieved 2011-07-05.

Hashemi, Hassan, et al. "Global and regional estimates of prevalence of refractive errors: systematic review and meta-analysis." *Journal of current ophthalmology* 30.1 (2018): 3-22.

Hatch BB, Moshirfar M, Ollerton AJ, Sikder S, Mifflin MD. A prospective, contralateral comparison of photorefractive keratectomy (PRK) versus thin-flap LASIK: assessment of visual function. *Clin Ophthalmol*. 2011;5:451-7. doi: 10.2147/OPHTH.S18967. Epub 2011 Apr 21. PMID: 21573091; PMCID: PMC3090298.

Heishma, Stephen J., Richard C. Taylor, and Jack E. Henningfield. "Nicotine and smoking: a review of effects on human performance." *Experimental and Clinical Psychopharmacology* 2.4 (1994): 345

Holden B, Sankaridurg P, Smith E, Aller T, Jong M, He M (February 2014). "Myopia, an underrated global challenge to vision: where the current data takes us on myopia control"

<https://www.who.int/mediacentre/news/releases/2006/pr55/en/>

Huang, X; He, X; Tan, X (2002). "Research of corneal ectasia following laser in-situ keratomileusis in rabbits". *Yan Ke Xue Bao*. 18 (2): 119–22. PMID 15510652.

Iribarren, Rafael, et al. "Crystalline lens power and refractive error." *Investigative ophthalmology & visual science* 53.2 (2012): 543-550

Kaplan, H. J. (2007). *Anatomy and Function of the Eye*. *Chemical Immunology and Allergy*, 4–10. doi:10.1159/000099236

Koch, DD (1997). "Excimer laser technology: new options coming to fruition". *Journal of Cataract and Refractive Surgery*. 23 (10): 1429–30. doi:10.1016/s0886-3350(97)80001-6. PMID 9480341.

Koch, DD; Kohnen, T; Obstbaum, SA; Rosen, ES (1998). "Format for reporting refractive surgical data". *Journal of Cataract and Refractive Surgery*. 24 (3): 285–7. doi:10.1016/s0886-3350(98)80305-2. PMID 9559453.

Kolb, Helga. "Simple anatomy of the retina." *Webvision: The organization of the retina and visual system* (1995): 13-36.

"LASIK Eye Surgery". TO VIMA, greek newspaper. 2009-10-11. Retrieved 2017-07-14.

"LASIK VS LASEK – A Comparison Chart". *The-lasik-directory.com*. Retrieved 2011-07-05

Li SM, Kang MT, Zhou Y, Wang NL, Lindsley K (2017). "Wavefront excimer laser refractive surgery for adults with refractive errors". *Cochrane Database Syst Rev*. 6 (6): CD012687. doi:10.1002/14651858.CD012687. PMC 6481747

Lowth, Mary. "Long Sight (Hypermetropia)". Patient. Patient Platform Limited. Archived from the original on 2016-03-03. Retrieved 2016-02-26.

Maggs, David J. "CORNEA AND SCLERA 10." *Slatter's fundamentals of veterinary ophthalmology* (2008): 175.

Maher, Sam, et al. *Nanostructured biomaterials for overcoming biological barriers*. Royal Society of Chemistry, 2012.

Manche, Edward E., and Weldon W. Haw. "Wavefront-guided laser in situ keratomileusis (Lasik) versus wavefront-guided photorefractive keratectomy (Prk): a prospective randomized eye-to-eye comparison (an American Ophthalmological Society thesis)." *Transactions of the American Ophthalmological Society* 109 (2011): 201.

Mastrangelo, Carlos, Nazmul Hasan, and Kim Hanseup. "Low-power large aperture adaptive lenses for smart eyeglasses." U.S. Patent Application No. 16/068,328.

Michelson, A. (1927). *Studies in Optics*. U. of Chicago Press. Ph.D., Lawrence Arend. "Luminance Contrast". colorusage.arc.nasa.gov. Retrieved 5 April 2018.

Moore, Bruce D.; Augsburger, Arol R.; Ciner, Elise B.; Cockrell, David A.; Fern, Karen D.; Harb, Elise (2008). "Optometric Clinical Practice Guideline: Care of the Patient with Hyperopia" (PDF). American

Morlet, N; Minassian, D; Dart, J (2002). "Astigmatism and the analysis of its surgical correction". *The British Journal of Ophthalmology*. 86 (12): 1458–9. doi:10.1136/bjo.86.12.1458. PMC 1771428. PMID 12446403

Munro BH. *Statistical Methods for Health Care Research*, 5th ed. Lippincott Williams & Wilkins, 2005.

Murueta-Goyena A, Cañadas P. Visual outcomes and management after corneal refractive surgery: A review. *J Optom*. 2018;11(2):121–129. doi:10.1016/j.optom.2017.09.002

Newsome, D.A., J. Gross, and J.R. Hassell, Human corneal stroma contains three distinct collagens. *Invest Ophthalmol Vis Sci*, 1982. 22(3): p. 376-81.

Nishida, Teruo, and Shizuya Saika. "Cornea and sclera: anatomy and physiology." *Cornea—Fundamentals, Diagnosis and Management*. Mosby Elsevier (2010): 3-24.

Ngoei, Enette (February 2013). "Refractive editor's corner of the world: CorT'ing accuracy". *EyeWorld*. Retrieved 22 April 2013.

Oyster, Clyde W. "The human eye." Sunderland, MA: Sinauer (1999).

Park, K. L. "Anatomy of the uvea." *Ophthalmology*. Mosby St. Louis (MO), 1999. 10-2.

Pathai, S; Shiels, PG; Lawn, SD; Cook, C; Gilbert, C (March 2013). "The eye as a model of ageing in translational research--molecular, epigenetic and clinical aspects". *Ageing Research Reviews*. 12 (2): 490–508. doi:10.1016/j.arr.2012.11.002. PMID 23274270

Pomerantzeff O, Pankratov M, Wang GJ, Dufault P. Wide-angle optical model of the eye. *Am J Optom Physiol Opt.* 1984;61(3):166-176.

Prince, Jerry L., Links, Jonathan M. *Medical Imaging Signals and Systems*, (2006). pg 65 Ch 3 Image Quality, 3.2 Contrast, 3.2.1 Modulation.

"Refractive Correction With C-TEN" (PDF). *Bmctoday*.

Remington, Lee Ann, and Denise Goodwin. *Clinical anatomy of the visual system E-Book*. Elsevier Health Sciences, 2011.

Richman, Jesse, et al. "The Spaeth/Richman contrast sensitivity test (SPARCS): design, reproducibility and ability to identify patients with glaucoma." *British Journal of Ophthalmology* 99.1 (2015): 16-20.

Richman, Jesse, George L. Spaeth, and Barbara Wirostko. "Contrast sensitivity basics and a critique of currently available tests." *Journal of Cataract & Refractive Surgery* 39.7 (2013): 1100-1106.

Richter GM, Wang M, Jiang X, et al. Ocular Determinants of Refractive Error and Its Age- and Sex-Related Variations in the Chinese American Eye Study. *JAMA Ophthalmol.* 2017;135(7):724–732. doi:10.1001/jamaophthalmol.2017.1176

Robert P. Rutstein, Kent M. Daum, *Anomalies of Binocular Vision: Diagnosis & Management*, Mosby, 1998.

Rosner BA. *Fundamentals of Biostatistics*, 4th ed. Duxbury, 1995.

Ross JE, Clarke DD, Bron AJ. Effect of age on contrast sensitivity function: uniocular and binocular findings. *Br J Ophthalmol.* 1985 Jan;69(1):51-6. doi: 10.1136/bjo.69.1.51. PMID: 3965028; PMCID: PMC1040522.

Rothman KJ, Greenland S. *Modern Epidemiology*, 2nd ed. Lippincot- Raven 1998.

Sakthivel, M., et al., Alterations in lenticular proteins during ageing and selenite-induced cataractogenesis in Wistar rats. *Mol Vis*, 2010. 16: p. 445-53.

Sand, J. P., Zhu, B. Z., & Desai, S. C. (2016). Surgical Anatomy of the Eyelids. *Facial Plastic Surgery Clinics of North America*, 24(2), 89–95. doi:10.1016/j.fsc.2015.12.001

Schiøtz, H. (1885). "Ein Fall von hochgradigem Hornhautastigmatismus nach Starextraktion: Besserung auf operativem Wege". *Arch Augenheilkd.* 15: 178–181.

Selhorst, John B., and Yanjun Chen. "The optic nerve." *Seminars in neurology*. Vol. 29. No. 01. © Thieme Medical Publishers, 2009.

Shedecor GW, Cochran WG. *Statistical Methods*, 8th ed. Iowa State Univ Press, 1989.

Silvestrini, T. A.; Pinsky, P. M.; Christie, B. (2005). "Analysis of Glucose Diffusion Across the Acufocus Corneal Inlay Using a Finite Element Method". *Investigative Ophthalmology & Visual Science*. 46 (5): 2195. Archived from the original on 2015-01-09.

Singer, J. D. & Willett, J. B. (2003). *Applied Longitudinal Data Analysis: Modeling Change and Event Occurrence*. Oxford University Press.

Solomon, KD; Fernández De Castro, LE; Sandoval, HP; Biber, JM; Groat, B; Neff, KD; Ying, MS; French, JW; Donnenfeld, ED (2009). "LASIK world literature review: Quality of life and patient satisfaction". *Ophthalmology*. 116 (4): 691–701. doi:10.1016/j.ophtha.2008.12.037. PMID 19344821.

Smith G, Atchinson DA. The eye. In: Smith G, Atchinson DA, eds. *The Eye and Visual Optical Instruments*. Cambridge, UK: Cambridge University Press; 1997:291-316.

Snijders, T. A. B. & Bosker, R. J. (2012). *Multilevel Analysis*, 2nd ed. Sage Publications.

Sridhar, Mittanamalli S. "Anatomy of cornea and ocular surface." *Indian journal of ophthalmology* 66.2 (2018): 190.

Stewart, Michael W. "The Diabetic Retina: Anatomy and Pathophysiology." *Diabetic Retinopathy*. Adis, Singapore, 2017. 29-72.

Stijnen T, Mulder PGH. Classical methods for data analyses. NIHES program, Rotterdam, 1999

Taylor, HR; Carson, CA (1994). "Excimer laser treatment for high and extreme myopia". Transactions of the American Ophthalmological Society. 92: 251–64, discussion 264–70. PMC 1298510. PMID 7886866.

Tear Film; in Basic and Clinical Science Course; Section 2: Fundamentals and Principles of Ophthalmology. San Francisco, American Academy of Ophthalmology, 2003–2004, pp 303–311.

The Cornea. Edited by: Kaufman, H., Barron, B., McDonald, M. Butterworth- Heinemann. Second Edition, 1998.

Thompson KP, Ren QS, Parel JM. Therapeutic and diagnostic application of lasers in ophthalmology. In: Waynant RW, ed. Lasers in Medicine. Boca Raton, FL: CRC Press. 2002:211-246.

Thumann, G., Development and cellular functions of the iris pigment epithelium. *Surv Ophthalmol*, 2001. 45(4): p. 345-54.

Vanston JE, Strother L. Sex differences in the human visual system. *J Neurosci Res*. 2017 Jan 2;95(1-2):617-625. doi: 10.1002/jnr.23895. PMID: 27870438

Vilensky, Joel A., Wendy Robertson, and Carlo A. Suarez-Quian. *The Clinical Anatomy of the Cranial Nerves: The Nerves of "On Old Olympus Towering Top"*. John Wiley & Sons, 2015.

Walsh G, Charman WN, Howland HC. Objective technique for the determination of monochromatic aberrations of the human eye. *J Opt Soc Am A*. 1984;1(9):987-992.

Wen D, McAlinden C, Flitcroft I, Tu R, Wang Q, Alió J, Marshall J, Huang Y, Song B, Hu L, Zhao Y, Zhu S, Gao R, Bao F, Yu A, Yu Y, Lian H, Huang J. Postoperative Efficacy, Predictability, Safety, and Visual Quality of Laser Corneal Refractive Surgery: A Network Meta-analysis. *Am J Ophthalmol*. 2017 Jun;178:65-78. doi: 10.1016/j.ajo.2017.03.013. Epub 2017 Mar 20. PMID: 28336402.

ABSTRACTS

Abstract

Objectives: To assess contrast sensitivity of central and peripheral vision with a newly developed internet-based Spaeth/Richman Contrast Sensitivity (SPARCS) test in subjects who underwent refractive surgery (PRK and femto-LASIK) for myopia in comparison to matched controls.

Methods: In this retrospective study, subjects who underwent a refractive surgery and normal controls were evaluated using the SPARCS. Contrast sensitivity testing was performed in each eye in a standardized testing environment in randomized order. SPARCS scores were obtained for central and 4 peripheral areas (right upper (RUQ), right lower (RLQ), left upper (LUQ), and left lower quadrants (LLQ)) and a new variable "peripheral" was created, which was the sum of 4 peripheral scores. Total, central and peripheral SPARCS scores in subjects with refractive surgery were compared with controls adjusting for possible confounders (age, gender, changed diopters, smoking). Univariate and multivariate linear regression and mixed linear regression were used.

Results: A total of 186 eyes from 93 subjects were analyzed: 62 eyes from 31 subjects at each of the 3 groups under comparison. The PRK group had a lower total score of 5.9 points (p -value <0.001), a lower central score of 1.6 points (p -value $=0.018$) and a lower peripheral score of 5.5 points (p -value $=0.006$) than the control group, but there was no statistically significant reduction in central and peripheral contrast sensitivity after LASIK compared to control group.

Conclusions: SPARCS offers the advantage of determining contrast sensitivity peripherally and centrally to patients that underwent a myopic refractive surgery. There was a statistically significant reduction in central and peripheral contrast sensitivity after PRK, but there was no statistically significant reduction in central and peripheral contrast sensitivity after femto-LASIK.

Περίληψη

Σκοπός: Να αξιολογηθεί η ευαισθησία αντίθεσης φωτεινότητας της κεντρικής και περιφερειακής όρασης με ένα πρόσφατα ανεπτυγμένο Spaeth / Richman (SPARCS) τεστ αντίθεσης φωτεινότητας που διενεργείται στο Διαδίκτυο σε άτομα που υποβλήθηκαν σε διαθλαστική χειρουργική επέμβαση (PRK και femto-LASIK) για τη διόρθωση μυωπίας σε σχέση με «υγιείς» μάρτυρες.

Μέθοδοι: Σε αυτήν την αναδρομική μελέτη, τα άτομα που υποβλήθηκαν σε διαθλαστική χειρουργική επέμβαση και οι μάρτυρες αξιολογήθηκαν χρησιμοποιώντας το SPARCS. Ο έλεγχος ευαισθησίας αντίθεσης πραγματοποιήθηκε σε κάθε μάτι σε τυποποιημένο περιβάλλον δοκιμών με τυχαία σειρά.

Λήφθηκαν βαθμολογίες SPARCS για την κεντρική και 4 περιφερειακές περιοχές (δεξιά πάνω (RUQ), δεξιά κάτω (RLQ), αριστερά άνω (LUQ) και αριστερά κάτω τεταρτημόρια (LLQ)) και δημιουργήθηκε μια νέα μεταβλητή "περιφερειακή", η οποία ήταν το άθροισμα των 4 περιφερειακών βαθμολογιών.

Συνολικά, οι κεντρικές και οι περιφερειακές βαθμολογίες του SPARCS σε άτομα με διαθλαστική

χειρουργική επέμβαση συγκρίθηκαν με αυτές των υγιων, έχοντας ελέγξει για συγχυτικούς παράγοντες (ηλικία, φύλο, αλλαγμένες διοπτρίες, κάπνισμα). Για την ανάλυσή μας χρησιμοποιήθηκαν μονοπαραγοντική και πολυπαραγοντική γραμμική παλινδρόμηση και μοντέλο μεικτών επιδράσεων.

Αποτελέσματα: Αναλύθηκαν συνολικά 186 μάτια από 93 άτομα: 62 μάτια από 31 άτομα σε κάθε μία από τις τρεις ομάδες σύγκρισης. Η ομάδα PRK είχε χαμηλότερη συνολική βαθμολογία 5,9 πόντων ($p < 0,001$), χαμηλότερη κεντρική βαθμολογία 1,6 πόντων (τιμή $p = 0,018$) και χαμηλότερη περιφερειακή βαθμολογία 5,5 πόντων ($p = 0,006$) από τον ομάδα μαρτύρων, αλλά δεν υπήρχε στατιστικά σημαντική μείωση στην ευαισθησία κεντρικής και περιφερειακής αντίθεσης φωτεινότητας μετά το LASIK σε σύγκριση με την ομάδα ελέγχου.

Συμπεράσματα: Το SPARCS προσφέρει το πλεονέκτημα του προσδιορισμού της ευαισθησίας αντίθεσης φωτεινότητας περιφερειακά και κεντρικά σε ασθενείς που υποβλήθηκαν σε διαθλαστική χειρουργική επέμβαση. Υπήρξε μια στατιστικά σημαντική μείωση της ευαισθησίας κεντρικής και περιφερειακής αντίθεσης μετά το PRK, αλλά δεν υπήρξε στατιστικά σημαντική μείωση της ευαισθησίας στην κεντρική και περιφερειακή αντίθεση μετά το femto-LASIK.

APPENDICES

DECLARATION FOR PARTICIPATION IN THE RESEARCH PROGRAM

You have been chosen to participate in a Research Program entitled: "Protocol of an epidemiological trial evaluating the difference of contrast sensitivity in individuals who underwent a refractive surgery", with lead researcher Tsiogka Anastasia and host the National and Kapodistrian University of Athens. The purpose of this study is to measure contrast sensitivity with a new method (SPARCS) in subjects undergoing laser-in-situ keratomileusis (LASIK), in subjects with photorefractive keratectomy (PRK) and in controls (persons who do not have a refractive error and have not undergone any refractive surgery). We want to study whether there are significant differences in Sparcs results between them. We will monitor 90 people in Athens for this survey. Demographic data will be recorded for all study participants: Demographic data (age, gender, occupation), ophthalmologic examination (visual acuity, ocular mobility, IOP, funduscopy), contrast sensitivity test score. The principle of confidentiality and anonymity will be respected for all information and data that we will collect, of course after your consent. Some of this data will be used for statistical analysis, scientific publications, and conference announcements completely anonymously and without ever disclosing or publishing your identity.

STATEMENT

I declare that I have read

the information above this document. The conditions, requirements, and benefits of this program have been understood. I therefore approve of my participation in the above research, as it contains, as designed by the competent body and the scientific researcher, knowing that it does not pose any risk to my physical and mental health. I also know that the program is free of charge and does not bring me any financial burden and that I can terminate my research at any time without any consequence.

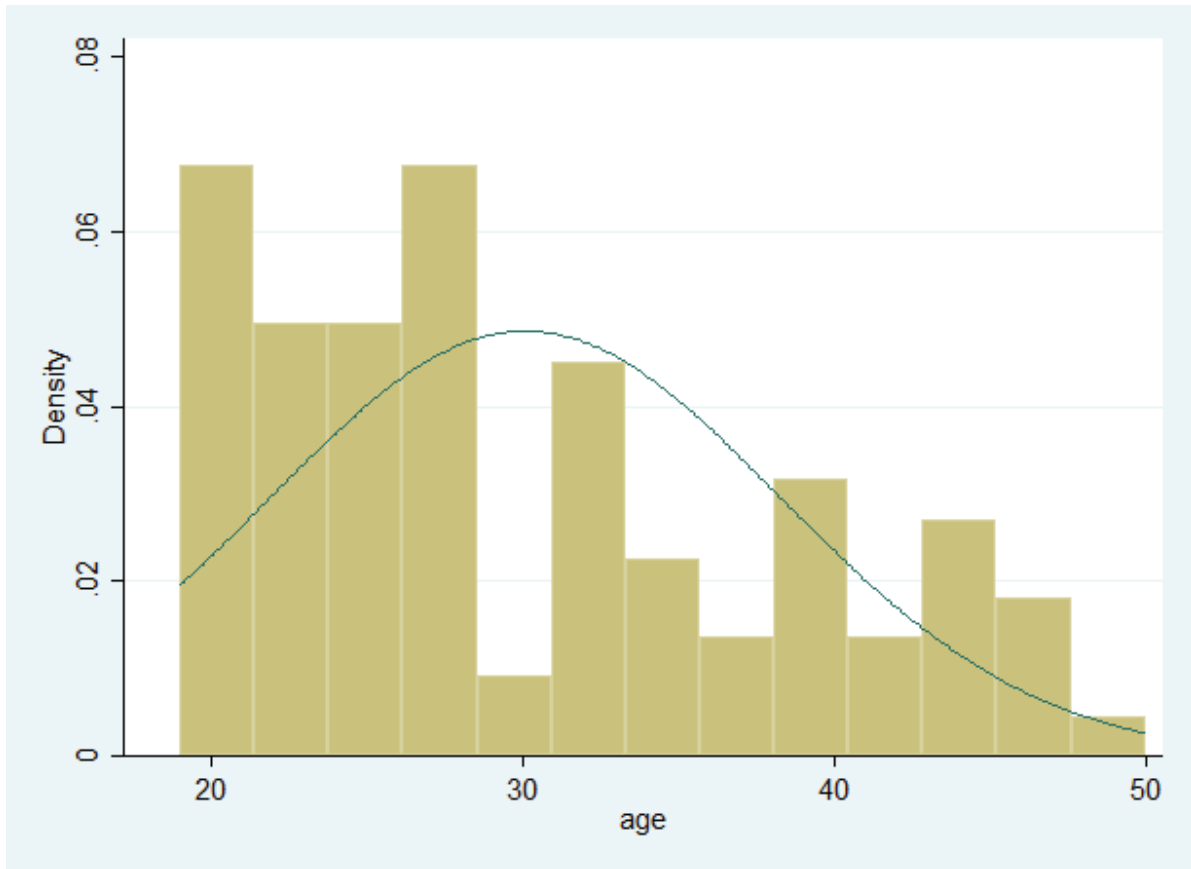
Date __ / __ / 20__

Signature

DATA DISTRIBUTION CHECKING

Shapiro-Wilk W test for normal data					
Variable	Obs	W	V	z	Prob>z
-----+-----					
age	186	0.92592	10.376	5.363	0.00000
One-sample Kolmogorov-Smirnov test against theoretical distribution					
normal((age-30.08602)/8.207651)					
Smaller group	D	P-value	Corrected		

age:	0.1734	0.000			
Cumulative:	-0.0988	0.026			
Combined K-S:	0.1734	0.000	0.000		

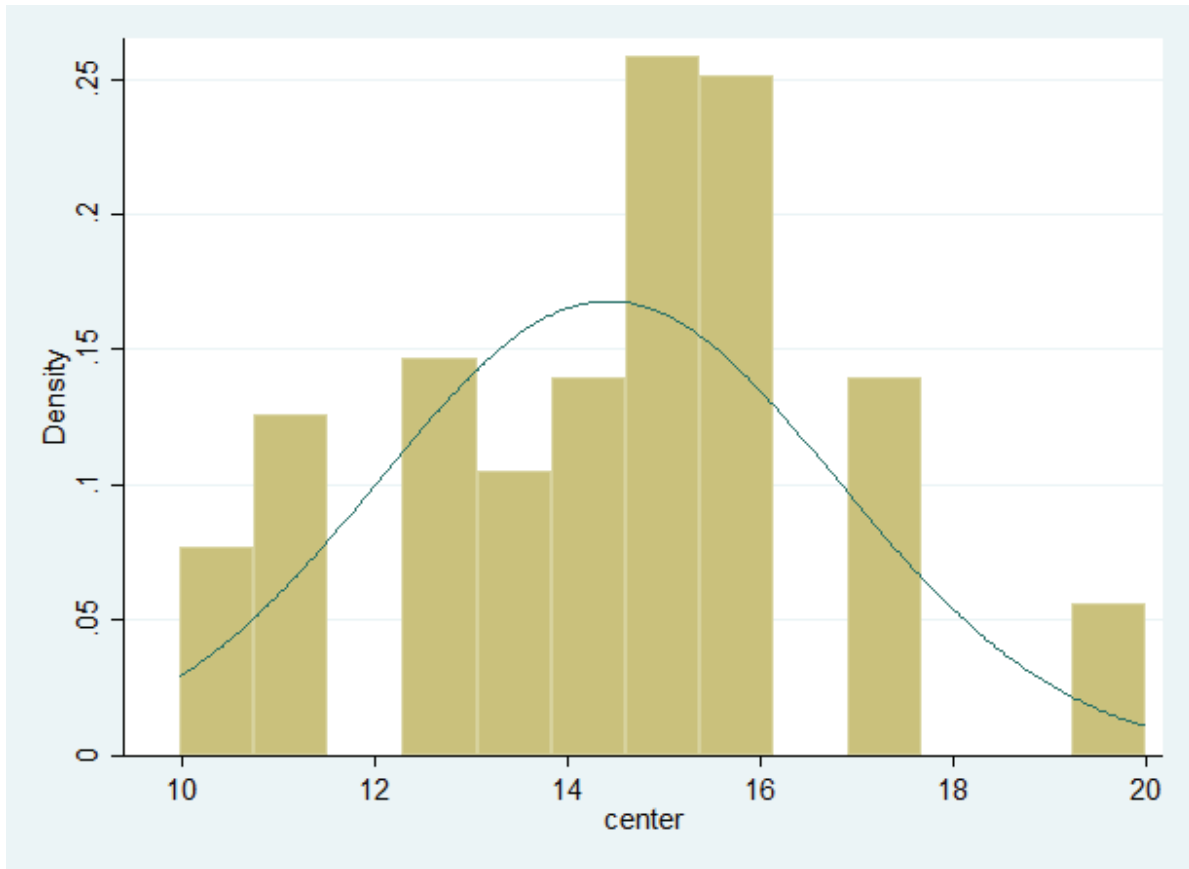


Shapiro-Wilk W test for normal data

Variable	Obs	W	V	z	Prob>z
center	186	0.99084	1.283	0.571	0.28385

One-sample Kolmogorov-Smirnov test against theoretical distribution
normal((center-14.42274)/ 2.375357)

Smaller group	D	P-value	Corrected
center:	0.1123	0.009	
Cumulative:	-0.1177	0.006	
Combined K-S:	0.1177	0.012	0.009



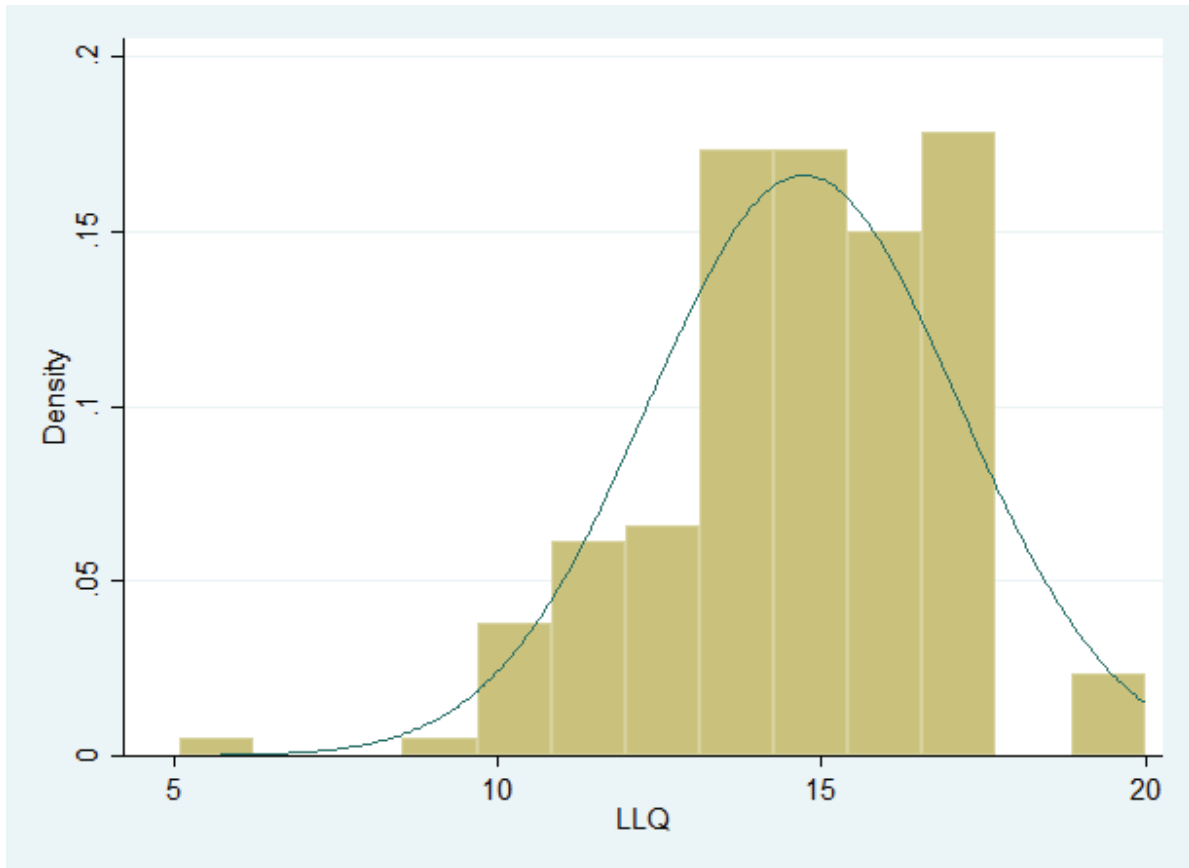
Shapiro-Wilk W test for normal data

Variable	Obs	W	V	z	Prob>z
LLQ	186	0.98082	2.686	2.265	0.01175

One-sample Kolmogorov-Smirnov test against theoretical distribution
normal((LLQ-14.72575)/ 2.402439)

Smaller group	D	P-value	Corrected
LLQ:	0.1033	0.019	
Cumulative:	-0.1153	0.007	

Combined K-S: 0.1153 0.014 0.011



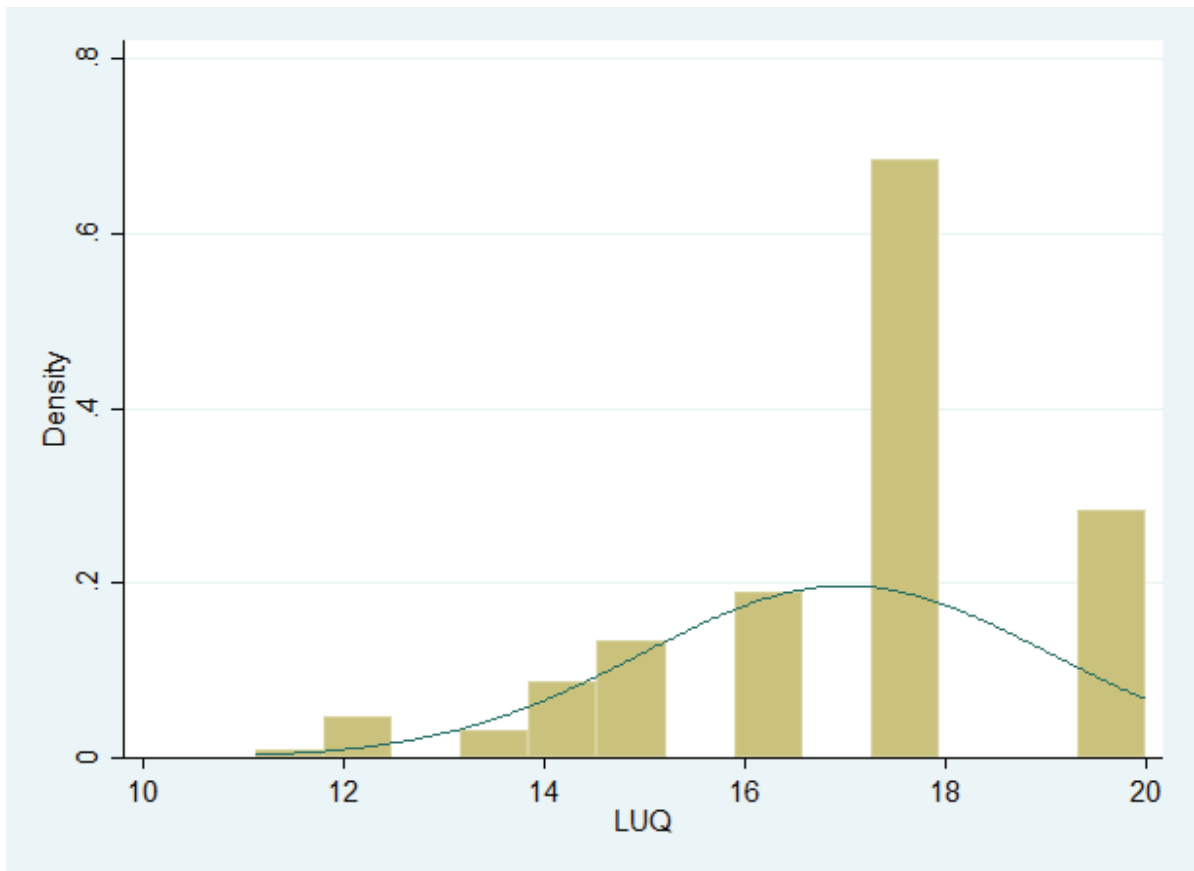
Shapiro-Wilk W test for normal data

Variable	Obs	W	V	z	Prob>z
LUQ	186	0.98481	2.128	1.731	0.04171

One-sample Kolmogorov-Smirnov test against theoretical distribution

normal((LUQ- 17.01269)/2.027994)

Smaller group	D	P-value	Corrected
LUQ:	0.2249	0.000	
Cumulative:	-0.2428	0.000	
Combined K-S:	0.2428	0.000	0.000



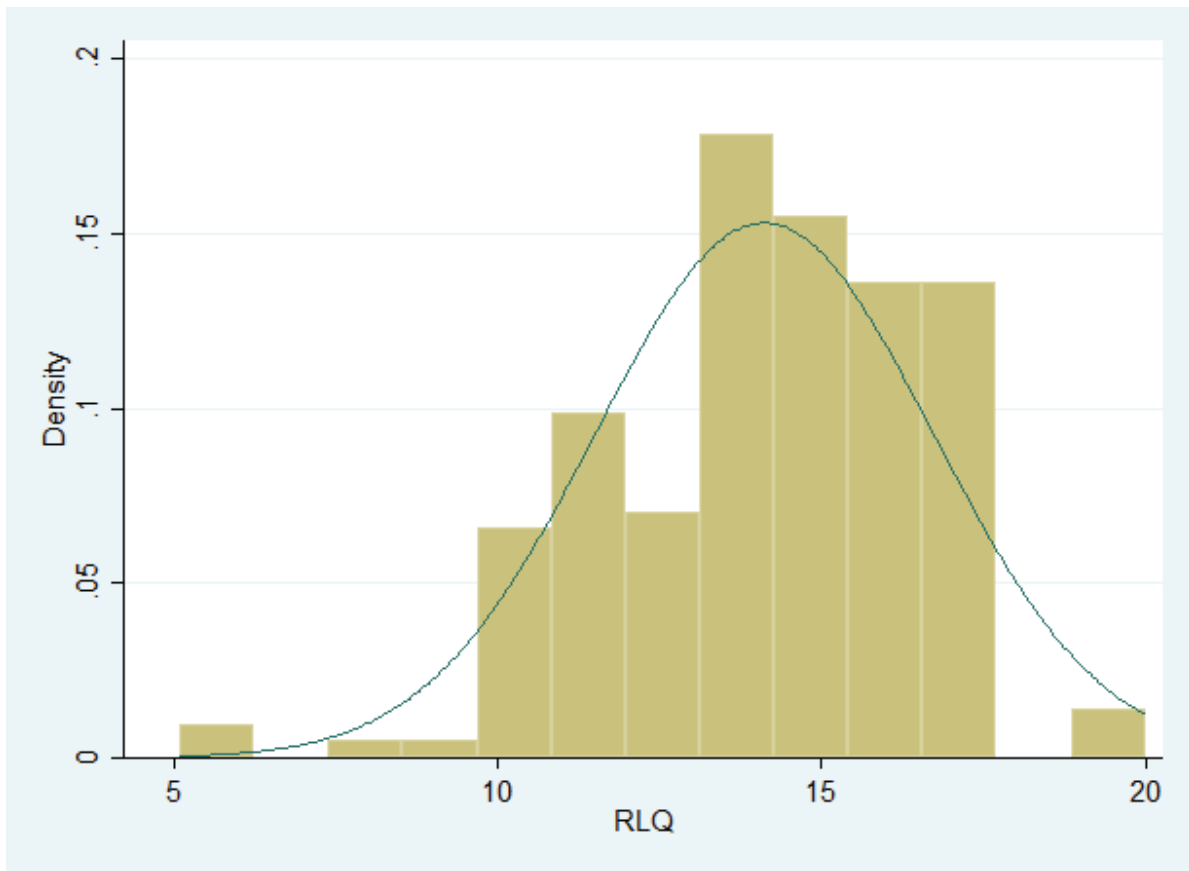
Shapiro-Wilk W test for normal data

Variable	Obs	W	V	z	Prob>z
RLQ	186	0.98168	2.566	2.160	0.01538

One-sample Kolmogorov-Smirnov test against theoretical distribution
normal((RLQ- 14.11425)/ 2.60637)

Smaller group	D	P-value	Corrected
RLQ:	0.0855	0.066	

Cumulative:	-0.1177	0.006	
Combined K-S:	0.1177	0.012	0.009

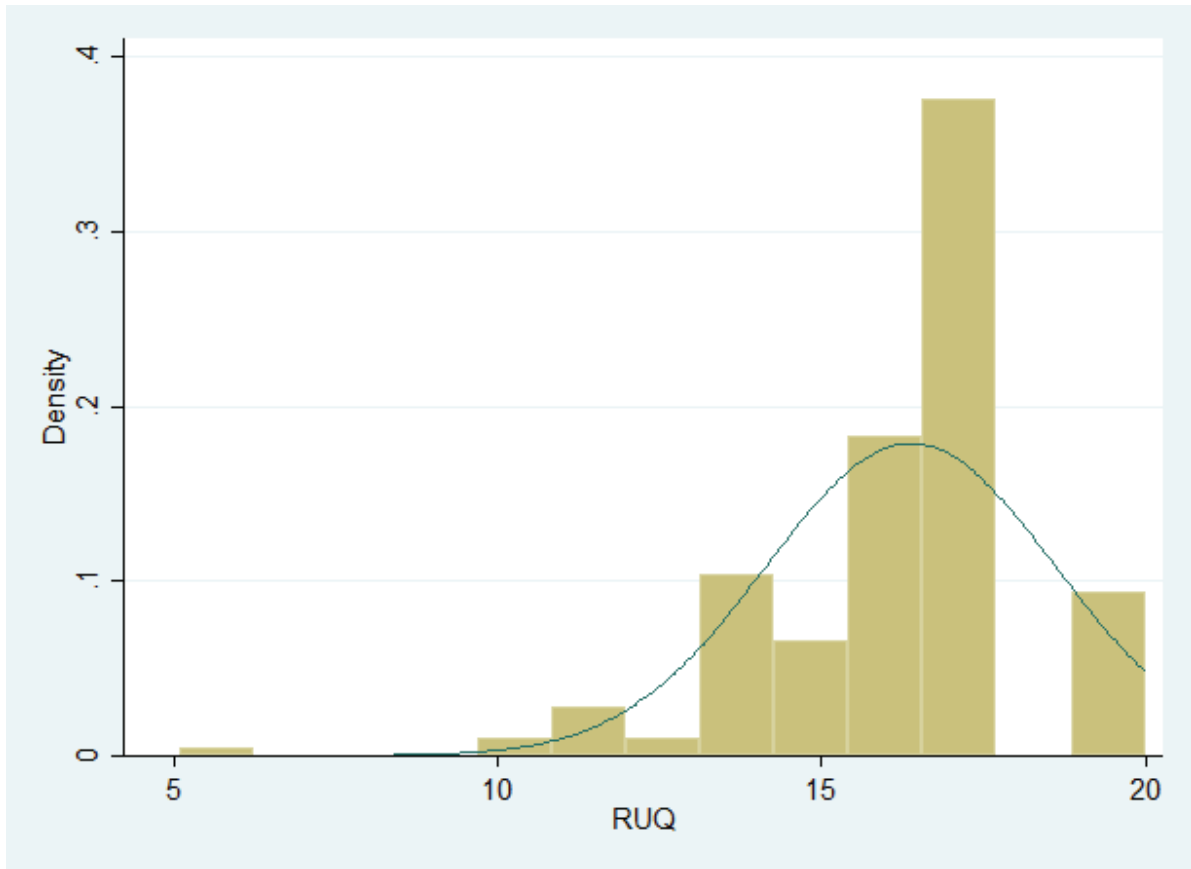


Shapiro-Wilk W test for normal data

Variable	Obs	W	V	z	Prob>z
RUQ	186	0.91950	11.276	5.554	0.00000

One-sample Kolmogorov-Smirnov test against theoretical distribution
normal((RUQ- 16.37629)/ 2.233617)

Smaller group	D	P-value	Corrected
RUQ:	0.2110	0.000	
Cumulative:	-0.2191	0.000	
Combined K-S:	0.2191	0.000	0.000

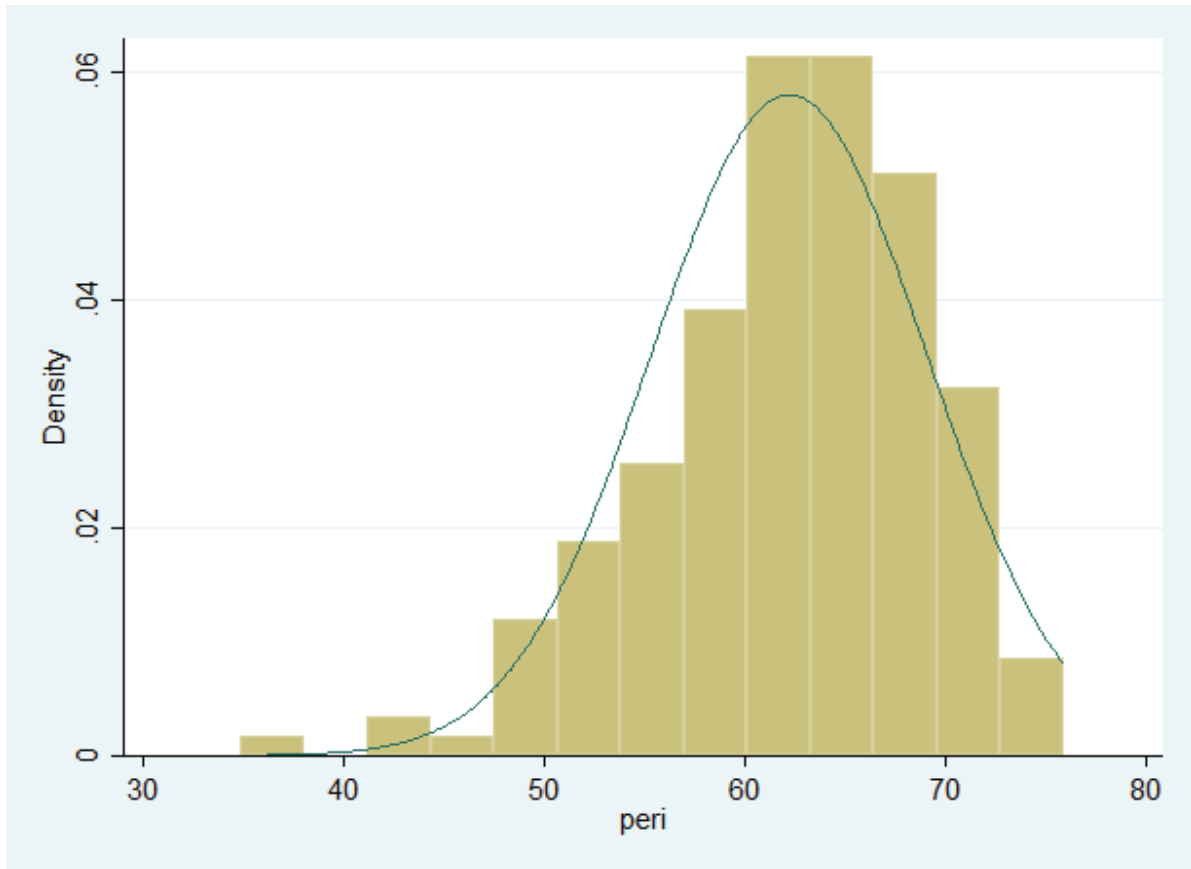


Shapiro-Wilk W test for normal data

Variable	Obs	W	V	z	Prob>z
peri	186	0.96689	4.637	3.517	0.00022

One-sample Kolmogorov-Smirnov test against theoretical distribution
normal((peri- 62.22898)/6.882209)

Smaller group	D	P-value	Corrected
peri:	0.0476	0.430	
Cumulative:	-0.0788	0.099	
Combined K-S:	0.0788	0.199	0.174

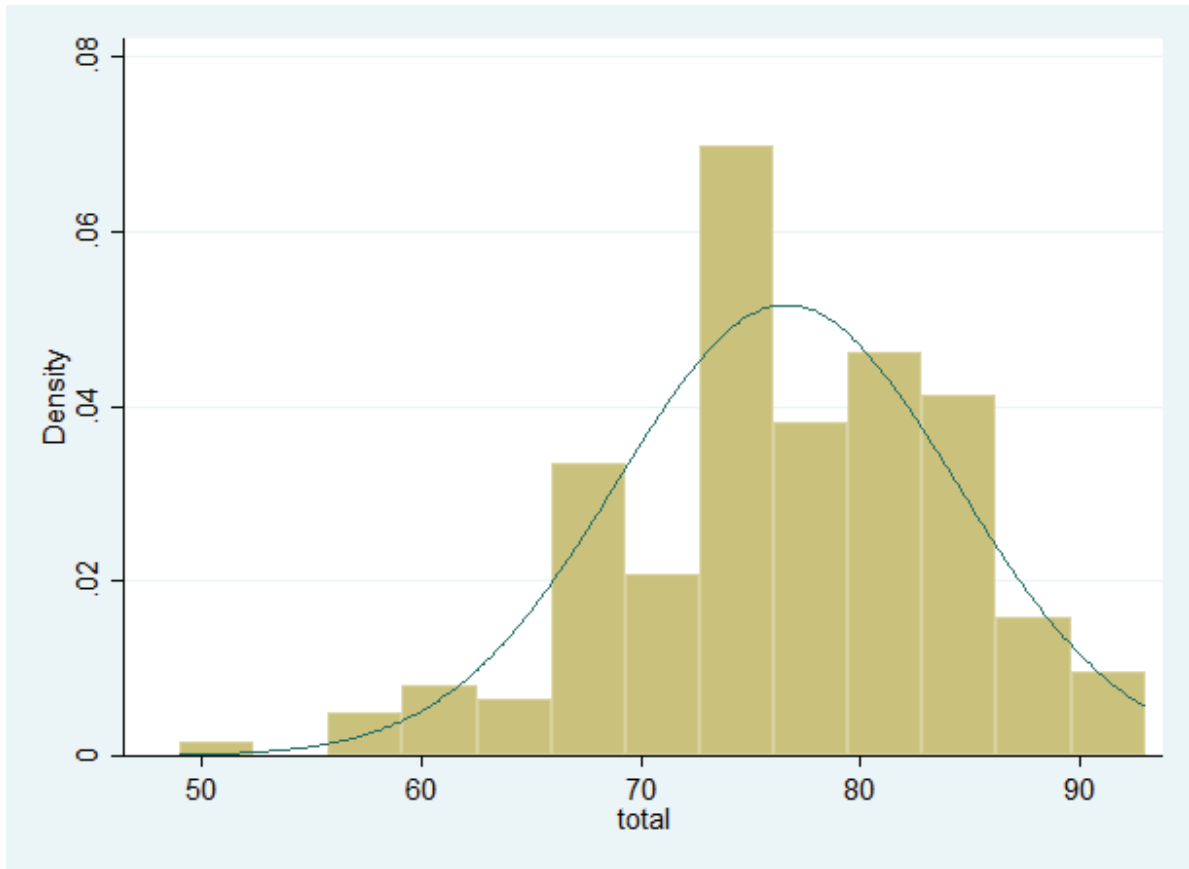


Shapiro-Wilk W test for normal data

Variable	Obs	W	V	z	Prob>z
total	186	0.98657	1.881	1.449	0.07369

One-sample Kolmogorov-Smirnov test against theoretical distribution
normal((tot- 76.63441)/ 7.730298)

Smaller group	D	P-value	Corrected
total:	0.0400	0.551	
Cumulative:	-0.0664	0.194	
Combined K-S:	0.0664	0.384	0.349

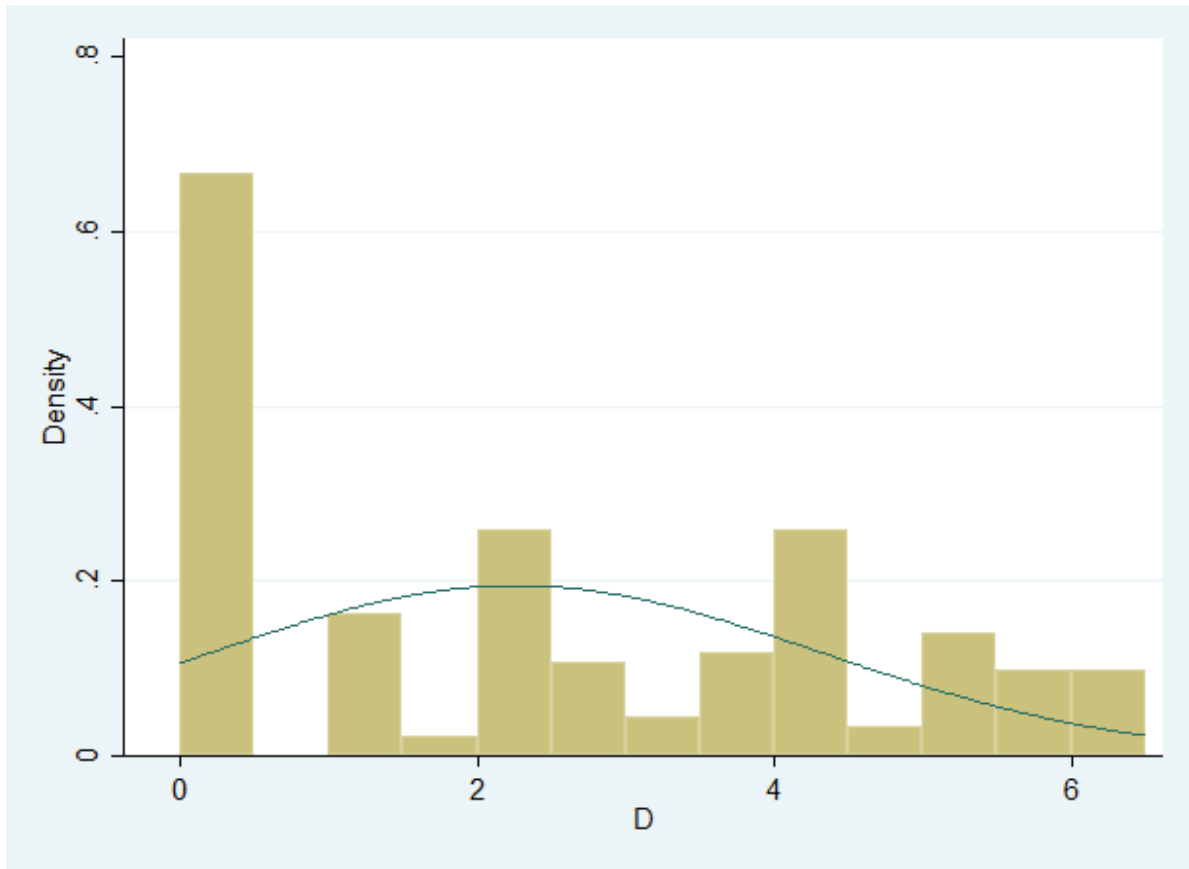


Shapiro-Wilk W test for normal data

Variable	Obs	W	V	z	Prob>z
D	186	0.94744	7.362	4.576	0.00000

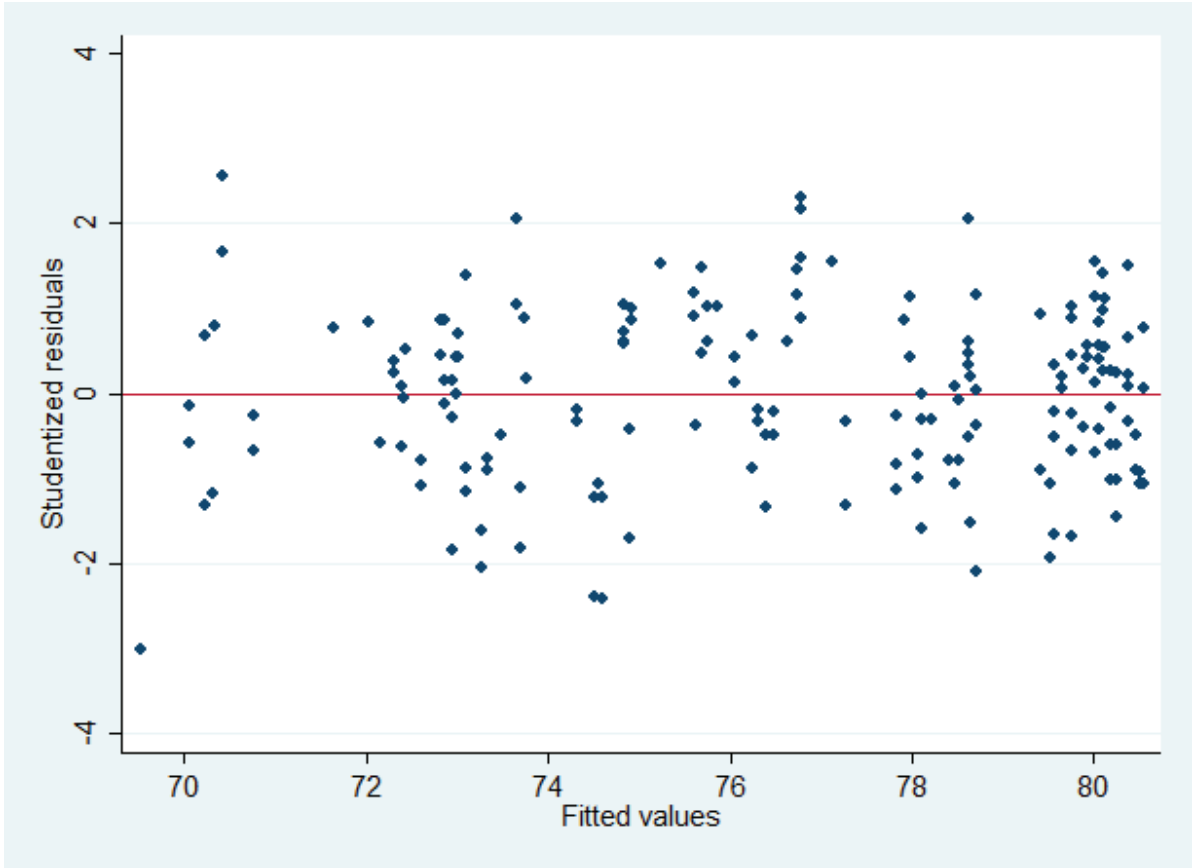
One-sample Kolmogorov-Smirnov test against theoretical distribution
normal((D- 2.260753)/ 2.048867)

Smaller group	D	P-value	Corrected
D:	0.1984	0.000	
Cumulative:	-0.1349	0.001	
Combined K-S:	0.1984	0.000	0.000

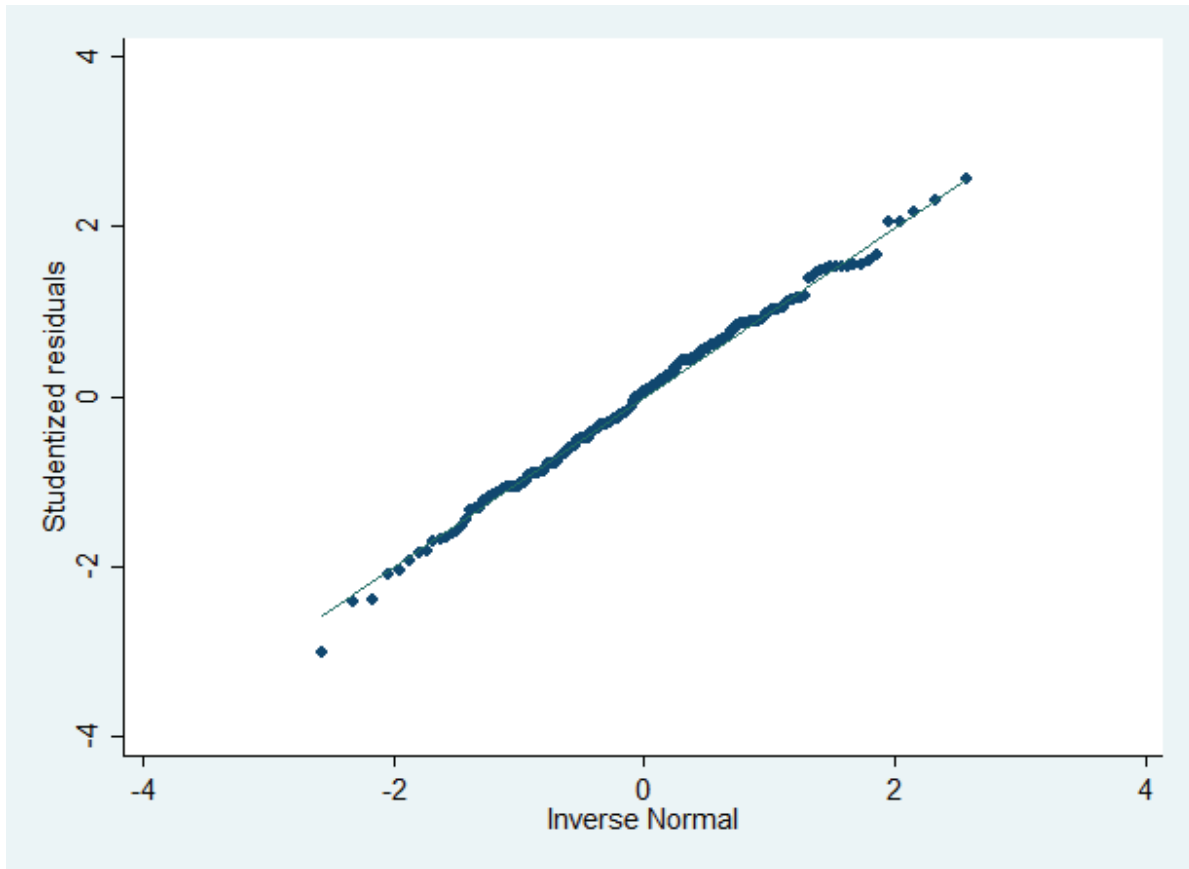


MODEL CHECKING

```
quietly xi: reg to age i.surg i.sex i.smok D
. predict yhat
. predict r, resid
. predict rstan,rstand
. predict rstud, rstud
. sc rstud yhat, yline(0) xlabel( ) ylabel( )
```



```
. qnorm rstud, xlab() ylab()
```



```
. swilk rstud
```

Shapiro-Wilk W test for normal data

Variable	Obs	W	V	z	Prob>z
rstud	186	0.99573	0.598	-1.180	0.88094

```
. predict d,cooksd
```

```
. predict h, hat
```

```
. list rstud d h if abs(rstud)>2.0 | h>.0382
```

	rstud	d	h
3.	1.66393	.0219209	.0530035

```

4. | 2.552841 .0505501 .0530035 |
5. | .7096297 .0033566 .0444602 |
6. | .4247166 .0012045 .0444602 |
7. | 1.040071 .0129537 .0773729 |
--Break--
. list rstud d h if abs(rstud)>2.0 & h>.0382

```

```

+-----+
|      rstud          d          h |
+-----+
4. | 2.552841 .0505501 .0530035 |
31. | -3.004009 .0705032 .0540525 |
150. | 2.056823 .0247255 .0399849 |
164. | -2.410092 .0482493 .0563441 |
176. | -2.401781 .0506909 .0593997 |
+-----+

```

```
. summarize d
```

```

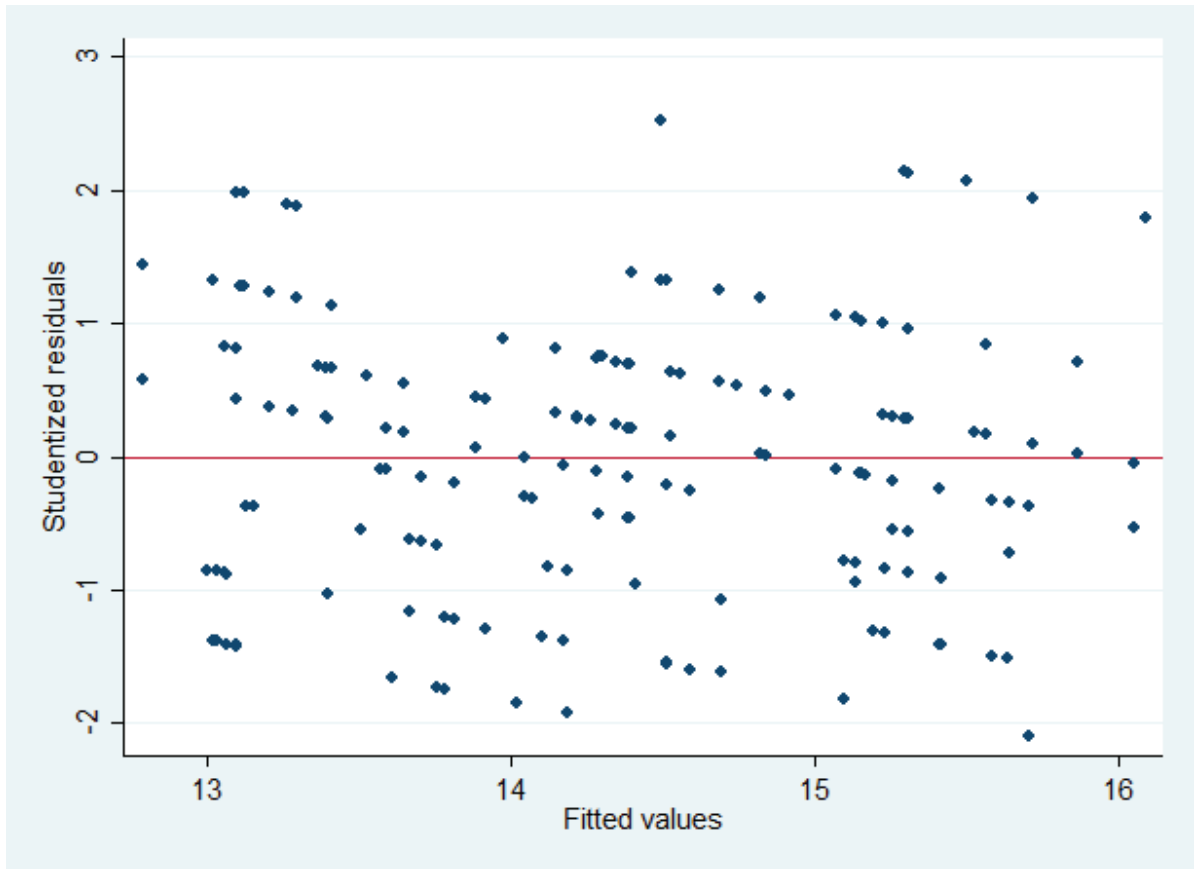
Variable |      Obs      Mean   Std. Dev.   Min      Max
-----+-----
d |      186   .0058556   .0094391  2.70e-08   .0705032

```

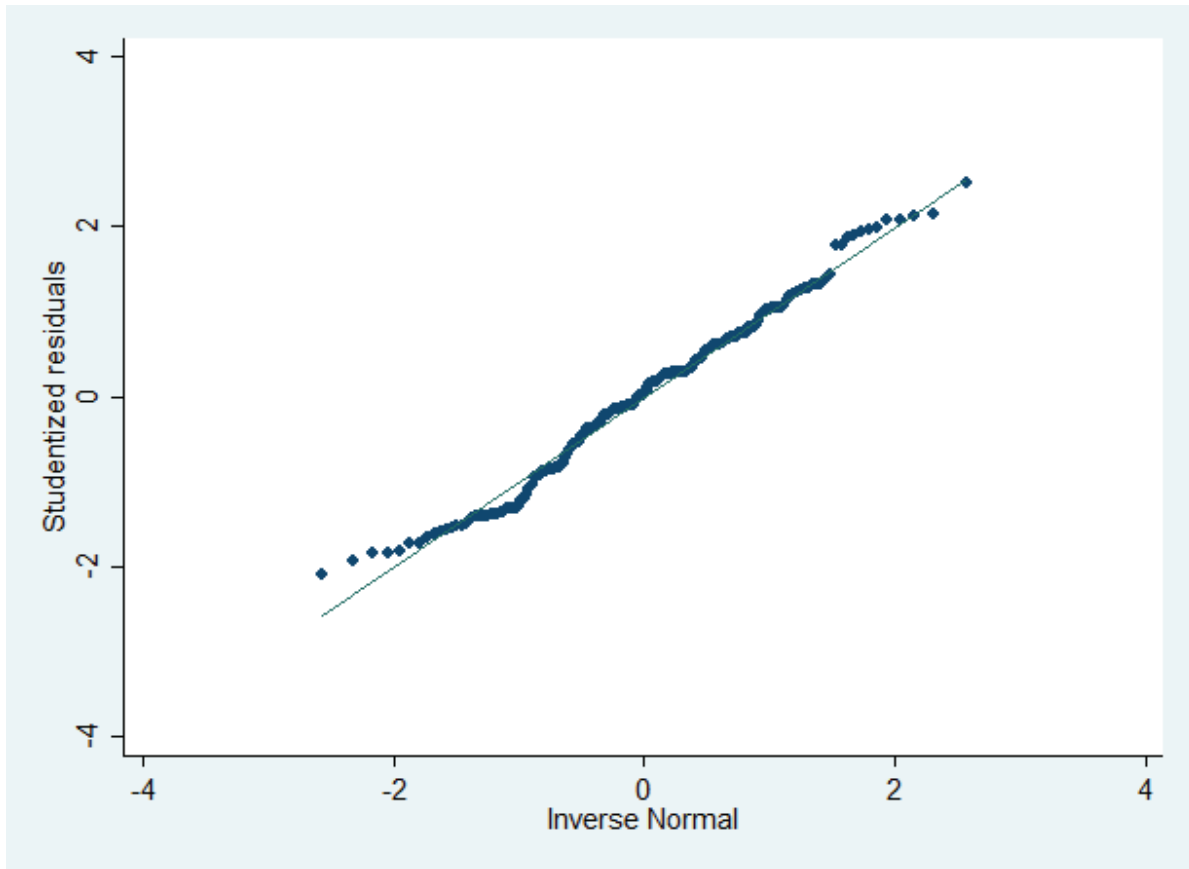
```

quietlyxi: reg ce age i.surg i.sex i.smok D
. predict yhat
. predict r, resid
. predict rstan,rstand
. predict rstud, rstud
. sc rstud yhat, yline(0) xlab( ) ylab( )

```



```
. qnorm rstud, xlab() ylab()
```



```
. swilk rstud
```

Shapiro-Wilk W test for normal data

Variable	Obs	W	V	z	Prob>z
rstud	186	0.98384	2.263	1.872	0.03059

```
. predict d,cooksd
```

```
. predict h, hat
```

```
. list rstud d h if abs(rstud)>2.0 | h>.0382
```

	rstud	d	h
3.	.5720704	.0026266	.0530035

```

4. | 1.440903 .0165015 .0530035 |
5. | .807134 .0043387 .0444602 |
6. | -1.420072 .0133287 .0444602 |
7. | -.4248873 .0021727 .0773729 |

. list rstud d h if abs(rstud)>2.0 & h>.0382

```

```

+-----+
|  rstud      d      h |
+-----+
111. | 2.074331 .0335358 .0526389 |
112. | 2.074331 .0335358 .0526389 |
+-----+

```

```

. summarize d

```

```

Variable |      Obs      Mean  Std. Dev.      Min      Max
-----+-----
d |      186   .0056023   .0070864  1.32e-08   .0335358

```

```

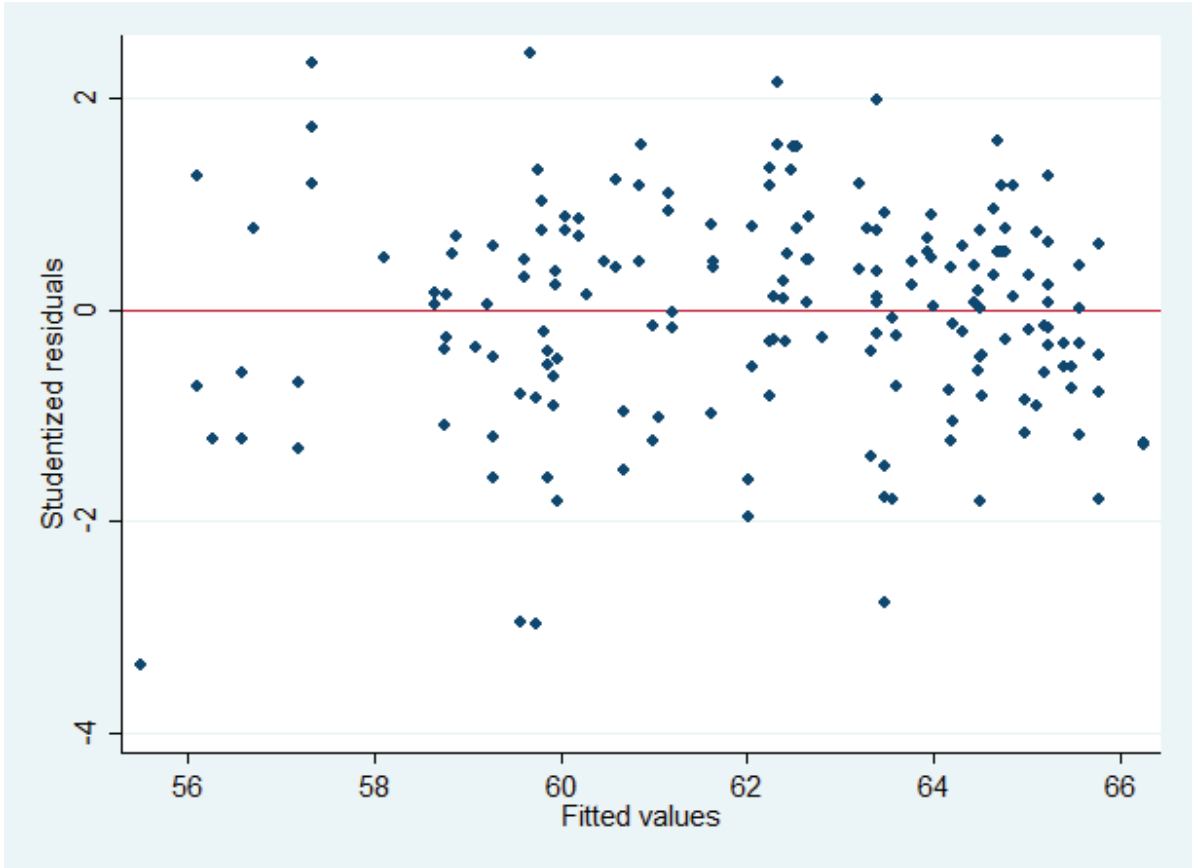
quietlyxi: reg peri age i.surg i.sex i.smok D

```

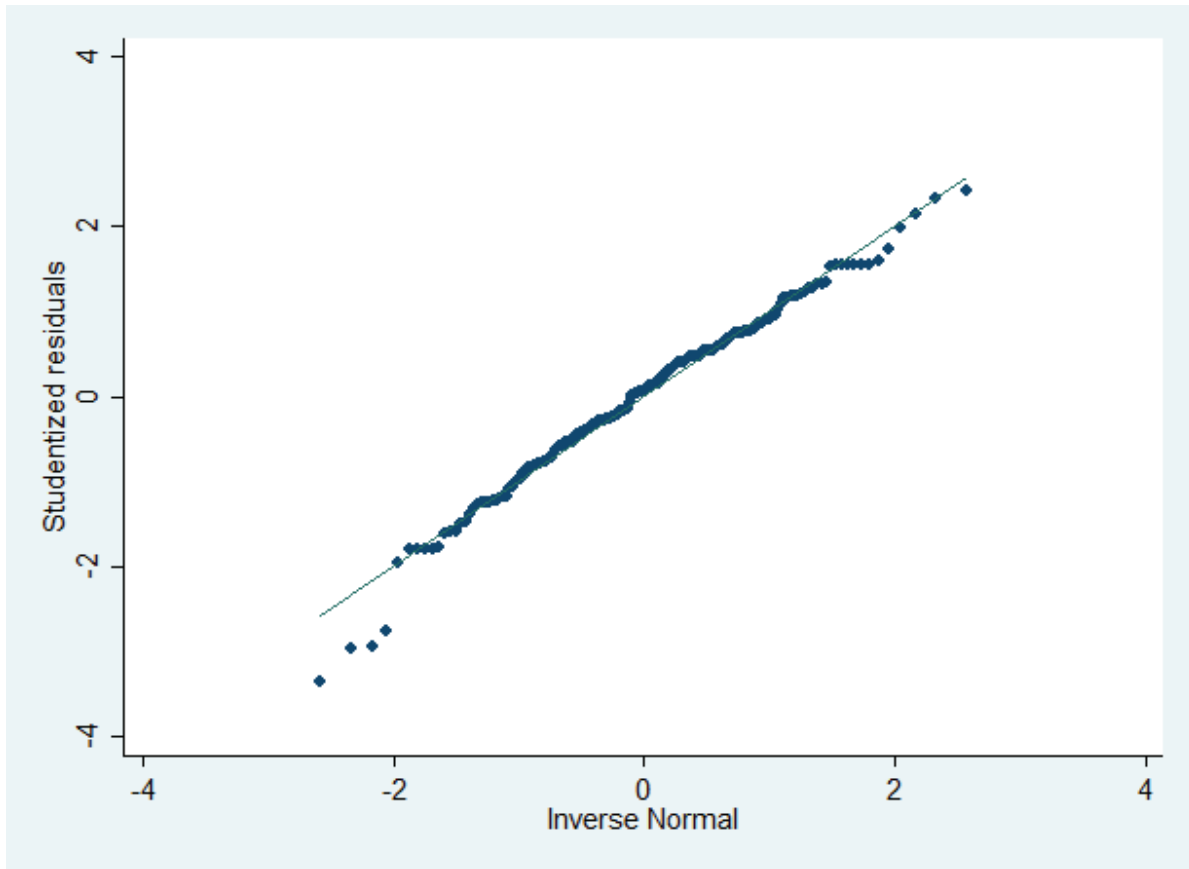
```

. predict yhat
. predict r, resid
. predict rstan,rstand
. predict rstud, rstud
. sc rstud yhat, yline(0) xlab( ) ylab( )

```



```
. qnorm rstud, xlab() ylab()
```



```
. swilk rstud
```

Shapiro-Wilk W test for normal data

Variable	Obs	W	V	z	Prob>z
rstud	186	0.98577	1.993	1.581	0.05693

```
. predict d,cooksd
```

```
. predict h, hat
```

```
. list rstud d h if abs(rstud)>2.0 | h>.0382
```

	rstud	d	h
3.	1.735206	.0238072	.0530035

```

4. | 2.328604 .0423107 .0530035 |
5. | .7506284 .0037544 .0444602 |
6. | 1.030754 .0070597 .0444602 |
7. | 1.226529 .0179721 .0773729 |

```

--Break--

```
. list rstud d h if abs(rstud)>2.0 & h>.0382
```

```

+-----+
|      rstud          d          h |
|-----|
4. | 2.328604 .0423107 .0530035 |
31. | -3.362205 .0872553 .0540525 |
150. | 2.421648 .0339702 .0399849 |
158. | -2.759076 .0509487 .0463294 |
164. | -2.974956 .0723197 .0563441 |
|-----|
176. | -2.951715 .0753545 .0593997 |
+-----+

```

```
. summarize d
```

```

Variable |      Obs      Mean  Std. Dev.      Min      Max
-----+-----
d |      186   .0062003      .

```



Π.Μ.Σ. ΒΙΟΣΤΑΤΙΣΤΙΚΗΣ

Συμμετέχοντα Τμήματα:

Ιατρική Σχολή Πανεπιστημίου Αθηνών
Μαθηματικών Πανεπιστημίου Αθηνών

ΒΕΒΑΙΩΣΗ

Ο μεταπτυχιακός φοιτητής ...Αναστασία Τσιώγκα..... ολοκλήρωσε τη διπλωματική εργασία του με τίτλο **An epidemiological study evaluating contrast sensitivity change in refractive surgery** στα πλαίσια των σπουδών του για το Διατμηματικό Μεταπτυχιακό Δίπλωμα Ειδίκευσης στη “Βιοστατιστική” των Τμημάτων Μαθηματικών και Ιατρικής Σχολής του Πανεπιστημίου Αθηνών.

Την εργασία αυτή παρουσίασε σε δημόσια διάλεξη στις ...28-01-2021... στο Τμήμα

...Βιοστατιστικής... του Πανεπιστημίου Αθηνών.

Μετά από προφορική εξέταση που ακολούθησε τη διάλεξη, η τριμελής εξεταστική επιτροπή, ενέκρινε ομόφωνα τη διπλωματική αυτή εργασία.

Η Εξεταστική Επιτροπή

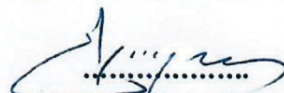
1. SAMOLI EVANGELIA

Assistant Professor of Epidemiology and
Medical Statistics, National and Kapodistrian
University of Athens


..... 24/2/21

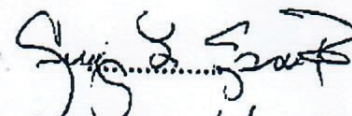
2. KARMIRIS EFTHYMIOS

Consultant Ophthalmologist,
Hellenic Air Force, Athens


23 Feb 2021

3. SPAETH GEORGE L.

Research Professor,
Wills Eye Hospital, Philadelphia


20 Feb 2021